J. Am. Chem. Soc. **2000,** *122,* 9793−9807

Thermal and Photochemical Reactions of Aluminum, Gallium, and Indium Atoms (M) in the Presence of Ammonia: Generation and Characterization of the Species $M{\cdot}NH_3$, $HMNH_2$, MNH_2, and H_2MNH_2

Hans-Jörg Himmel,* Anthony J. Downs, and Tim M. Greene

Contribution from the Inorganic Chemistry Laboratory, University of Oxford,
South Parks Road, Oxford OX1 3QR, U.K.

Received April 14, 2000

Abstract: Isolation of aluminum, gallium, and indium atoms together with ammonia in a solid argon matrix is shown to result in a thermal reaction yielding the metal atom complex $Al{\cdot}NH_3$, $Ga{\cdot}NH_3$, or $In{\cdot}NH_3$, which has been characterized by its IR and UV−visible spectra. Upon photoactivation at $\lambda = 436$ nm, the metal atom inserts into an N−H bond of ammonia to form the divalent compound $HMNH_2$ (M = Al, Ga, or In). This product is photolabile, decomposing to the corresponding monovalent compound MNH_2 on exposure to broad-band UV−visible light ($200 \leq \lambda \leq 800$ nm). All the molecules have been identified by means of their IR spectra, the assignments being underwritten by the effects of D and ^{15}N substitution, and also by comparison either with the vibrational properties of known, related molecules or with those predicted by quantum chemical (DFT) calculations. The resulting analysis is elaborated for the light it sheds on the structures and electronic properties of the molecules.

Introduction

Compounds containing the group 13 metals bound to nitrogen are potentially relevant to the fabrication of the III−V semiconductor materials AlN, GaN, and InN.[1] In practice, these materials are made by organometallic chemical vapor deposition (OMCVD) processes starting from sources such as $Ga(CH_3)_3$ and NH_3.[1] The vapors of the precursors in H_2 as the carrier gas react at high temperatures at the substrate surface with the deposition of the metal nitride. Since hydrogen is one of the main impurities in the bulk material, the influence of hydrogen on the properties of the semiconductor device has been the subject of no little study.[2] The decomposition process is likely to proceed by way of intermediates with the composition $H_xM_yN_z$ (M = Al, Ga, or In); indeed the specific compounds amidogallane, $[H_2GaNH_2]_3$,[3] and azidogallane, $[H_2GaN_3]_n$,[4] are reported to be ready sources of GaN in cubic nanocrystalline form and thin films, respectively. Studies of a different kind involving high-resolution electron loss spectroscopy (HREELS), low energy electron diffraction (LEED), and other techniques show that adsorption of hydrogen atoms results in the creation on the GaN (0001) surface of Ga−H bonds that are destroyed only on heating to temperatures of 260 °C or higher.[5] It follows that detailed investigation of species with the general formula $H_xM_yN_z$ may be expected to illuminate our understanding not only of the decomposition processes implicated in the OMCVD formation of the binary nitride MN, but also of the factors affecting the properties of the product.

Matrix isolation is now well established as a highly instructive method of reconnaissance and characterization for previously unknown hydride derivatives of the group 13 metals.[6,7] Hence, for example, the simple monomeric molecule amidoborane, H_2BNH_2, has been identified as a product arising from the pyrolysis of mixtures of diborane and ammonia.[8,9] Moreover, the reactions of the metal atoms with dihydrogen molecules or hydrogen atoms have been shown to afford the first clear sighting of the binary hydride molecules MH, MH_2, and MH_3 (M = Al, Ga, or In).[10] Photoexcitation of the metal atoms is needed to promote insertion not only into the H−H bond of dihydrogen to give MH_2,[10] but also into a C−H bond of methane

---

* To whom correspondence should be addressed.

(1) Downs, A. J., Ed. *Chemistry of Aluminium, Gallium, Indium and Thallium*; Blackie: Glasgow, U.K., 1993. Edgar, J. H., Ed. *Properties of Group III Nitrides*; EMIS: London, U.K., 1994.

(2) Yu, Z.; Buczkowski, S. L.; Giles, N. C.; Myers, T. H.; Richards-Babb, M. R. *Appl. Phys. Lett.* **1996**, *69*, 2731−2733. Han, J.; Ng, T.-B.; Biefeld, R. M.; Crawford, M. H.; Follstaedt, D. M. *Appl. Phys. Lett.* **1997**, *71*, 3114−3116. Koleske, D. D.; Wickenden, A. E.; Henry, R. L.; Twigg, M. E.; Culbertson, J. C.; Gorman, R. J. *Appl. Phys. Lett.* **1998**, *73*, 2018−2020. Nakamura, S.; Iwasa, N.; Senoh, M.; Mukai, T. *Jpn. J. Appl. Phys., Part 1* **1992**, *31*, 1258−1266. Pearton, S. J.; Abernathy, C. R.; Ren, F.; Lothian, J. R.; Wisk, P. W.; Katz, A.; Constantine, C. *Semicond. Sci. Technol.* **1993**, *8*, 310−312.

(3) Hwang, J.-W.; Campbell, J. P.; Kozubowski, J.; Hanson, S. A.; Evans, J. F.; Gladfelter, W. L. *Chem. Mater.* **1995**, *7*, 517−525. Campbell, J. P.; Hwang, J.-W.; Young, V. G., Jr.; Von Dreele, R. B.; Cramer, C. J.; Gladfelter, W. L. *J. Am. Chem. Soc.* **1998**, *120*, 521−531.

(4) McMurran, J.; Kouvetakis, J.; Nesting, D. C.; Smith, D. J.; Hubbard, J. L. *J. Am. Chem. Soc.* **1998**, *120*, 5233−5237. McMurran, J.; Dai, D.; Balasubramanian, K.; Steffek, C.; Kouvetakis, J.; Hubbard, J. L. *Inorg. Chem.* **1998**, *37*, 6638−6644.

(5) Bellitto, V. J.; Thoms, B. D.; Koleske, D. D.; Wickenden, A. E.; Henry, R. L. *Surf. Sci.* **1999**, *430*, 80−88. Bellitto, V. J.; Yang, Y.; Thoms, B. D.; Koleske, D. D.; Wickenden, A. E.; Henry, R. L. *Surf. Sci.* **1999**, *442*, L1019−L1023.

(6) Almond, M. J.; Downs, A. J. *Adv. Spectrosc.* **1989**, *17*, 1−511. Downs, A. J.; Greene, T. M. *Adv. Inorg. Chem.* **1998**, *46*, 101−171.

(7) Downs, A. J. *Coord. Chem. Rev.* **1999**, *189*, 59−100.

(8) Carpenter, J. D.; Ault, B. S. *J. Phys. Chem.* **1991**, *95*, 3502−3506; *Chem. Phys. Lett.* **1992**, *197*, 171−174. Sugie, M.; Takeo, H.; Matsumura, C. *Chem. Phys. Lett.* **1979**, *64*, 573−575.

(9) McKee, M. L. *J. Phys. Chem.* **1992**, *96*, 5380−5385.

(10) Pullumbi, P.; Mijoule, C.; Manceron, L.; Bouteiller, Y. *Chem. Phys.* **1994**, *185*, 13−24. Pullumbi, P.; Bouteiller, Y.; Manceron, L.; Mijoule, C. *Chem. Phys.* **1994**, *185*, 25−37.

10.1021/ja001313x CCC: $19.00

to give CH_3MH (M = Al,[11] Ga[12−14] or In[14]); these divalent products are themselves photolabile, decomposing with the release of H atoms and the formation of the appropriate monovalent derivative (eq 1). The only insertion reactions of gallium and indium that have been found to proceed *without* photoactivation are those with HCl to give MCl and MH (M = Ga or In, although MH could be detected only for M = Ga)[15] and H_2, which reacts spontaneously with the Ga_2 dimer to give the hydrido-bridged species $Ga(\mu\text{-}H)_2Ga$.[13,16,17]

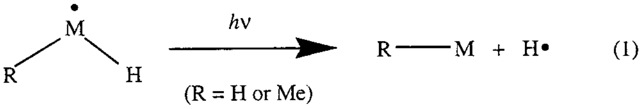

(1)

Here we report on the outcome of the reactions set in train by thermal or photolytic excitation of gallium or indium atoms isolated in ammonia-doped argon matrices. Previous studies of the reactions occurring between aluminum and ammonia in solid adamantane or argon matrices have been guided by EPR[18] or IR[19] measurements, respectively. The EPR experiments find evidence of the adducts $Al(NH_3)_2$ and $Al(NH_3)_4$ and what was thought to be the insertion product $HAlNH_2$, apparently featuring a bridging hydrogen atom, all formed by thermal reactions of ground-state Al atoms.[18] On the evidence of the IR experiments, Al atoms produced by laser ablation (and therefore including a proportion of electronically excited atoms) react with NH_3 to form two major products $HAlNH_2$ and $AlNH_2$, as well as another minor product tentatively identified as HAlNH.[19] These experiments indicated too that electronic excitation of the Al atoms is a prerequisite to insertion into an N−H bond of the NH_3 molecule, while offering no suggestion that the primary product $HAlNH_2$ carries other than terminal Al−H and N−H bonds. Photodecomposition of $HAlNH_2$ is then the source of the other two products. EPR studies of the reaction of Li atoms with NH_3 have identified the formation of the molecular complex $Li\cdot NH_3$, which decomposes under the action of visible light, possibly with the formation of $LiNH_2$ and LiNH, although these could not be positively identified.[20] Matrix methods have also been used to investigate the reactions of certain transition metals with ammonia. Thus, Fe[21] and Ni[22] atoms severally form adducts with one or two molecules of NH_3, and UV irradiation brings about insertion of the metal into an N−H bond with the formation of the amido derivatives $HMNH_2$ and $HMNH_2\cdot NH_3$ (M = Fe or Ni).

Ammonia complexes and amido and imido derivatives of aluminum have attracted several quantum chemical inquiries designed to elucidate the ground-state structures, vibrational properties, energetics, and, in particular, the bonding in such molecules.[7,23−28] As expected, the adducts $Al\cdot NH_3$[23,24] and $H_3Al\cdot NH_3$[24,25] are calculated to differ markedly in their binding energies (27−40 vs ca. 110 kJ mol^{-1}) and Al−N distances (2.350 vs 2.072 Å). $Al\cdot NH_3$ is noteworthy on two counts: (i) it is subject to Jahn−Teller distortion, albeit with minimal perturbation of the geometry and vibrational properties of the molecule (reflecting the highly localized character of the semioccupied orbital), and (ii) it is 110 kJ less stable than its tautomer $HAlNH_2$.[24] With a planar structure and a relatively short Al−N bond (1.772 Å), $HAlNH_2$ represents the global minimum for molecules with the composition $AlNH_3$. The most stable $AlNH_2$ isomer is not the quasi-linear HAlNH but the planar aluminum(I) species $AlNH_2$, also with a surprisingly short Al−N bond (1.795 Å);[24] together with an H atom this is formed from $HAlNH_2$ in a reaction analogous to eq 1 that is estimated to be exothermic by about 170 kJ mol^{-1}. Shortest of all are the Al−N bonds in the high-energy HAlNH (1.608 Å)[24−27] and the low-energy, planar H_2AlNH_2 molecule (1.766 Å)[24−26] for which the barrier to rotation about the Al−N bond is calculated[28] to be 45−60 kJ mol^{-1} (cf. 160 kJ mol^{-1} for H_2BNH_2[9]). There are signs therefore suggesting a degree of multiple bonding, but the precise nature and importance of such bonding are open to question.[7,29] Beyond doubt, however, is the need for more experimental facts not only about these, but also about the corresponding derivatives of gallium and indium, virtually uncharted up to the present time.

We will show that aluminum, gallium, and indium atoms in their ^2P ground states form relatively well-defined complexes $M\cdot NH_3$ (M = Al, Ga, or In) on co-condensation with ammonia. The complexes are characterized by distinctive UV−vis absorptions near 440 nm, irradiation into which brings about tautomerization to yield the divalent insertion product $HMNH_2$. This is not photostable but decomposes on exposure to broadband UV−visible light (λ = 200−800 nm) giving place to the univalent species MNH_2. Additionally, the released H atoms react with $HMNH_2$ to yield H_2MNH_2. Some of the results have been outlined in a preliminary communication.[30] The course of events as they occur in solid argon matrices at ca. 12 K has been tracked through the IR and UV−vis spectra of the matrices, and the identities of the products have been confirmed (i) by the response of the IR bands to isotopic enrichment in D or ^{15}N, (ii) by comparison with the results of density functional theory (DFT) calculations, and (iii) by reference to the properties of known cognate molecules. The properties observed or forecast for $M\cdot NH_3$, $HMNH_2$, MNH_2, H_2MNH_2, and related molecules invite comparisons, particularly for the light they shed on the characters of the M−N bonds. The findings are analyzed too in relation to the experimental circumstances for insights into the mechanisms of the photochemical changes.

---

(11) Parnis, J. M.; Ozin, G. A. *J. Phys. Chem.* **1989**, *93*, 1204−1215, 1220−1225.

(12) Xiao, Z. L.; Hauge, R. H.; Margrave, J. L. *Inorg. Chem.* **1993**, *32*, 642−646.

(13) Lafleur, R. D.; Parnis, J. M. *J. Phys. Chem.* **1992**, *96*, 2429−2433.

(14) Himmel, H.-J.; Downs, A. J.; Greene, T. M.; Andrews, L. *J. Chem. Soc., Chem. Commun.* **1999**, 2243−2244; *Organometallics* **2000**, *19*, 1060−1070.

(15) Himmel, H.-J.; Downs, A. J.; Greene, T. M. *J. Am. Chem. Soc.* **2000**, *122*, 922−930.

(16) Manceron, L., private communication.

(17) Himmel, H.-J.; Downs, A. J.; Greene, T. M., unpublished results.

(18) Howard, J. A.; Joly, H. A.; Edwards, P. P.; Singer, R. J.; Logan, D. E. *J. Am. Chem. Soc.* **1992**, *114*, 474−477.

(19) Lanzisera, D. V.; Andrews, L. *J. Phys. Chem. A* **1997**, *101*, 5082−5089.

(20) Meier, P. F.; Hauge, R. H.; Margrave, J. L. *J. Am. Chem. Soc.* **1978**, *100*, 2108−2112.

(21) Kauffman, J. W.; Hauge, R. H.; Margrave, J. L. *High Temp. Sci.* **1984**, *17*, 237−249. Szczepanski, J.; Szczesniak, M.; Vala, M. *Chem. Phys. Lett.* **1989**, *162*, 123−126.

(22) Ball, D. W.; Hauge, R. H.; Margrave, J. L. *High Temp. Sci.* **1988**, *25*, 95−101.

(23) Sakai, S. *J. Phys. Chem.* **1992**, *96*, 8369−8373.

(24) Davy, R. D.; Jaffrey, K. L. *J. Phys. Chem.* **1994**, *98*, 8930−8936.

(25) Marsh, C. M. B.; Hamilton, T. P.; Xie, Y.; Schaefer, H. F., III. *J. Chem. Phys.* **1992**, *96*, 5310−5317.

(26) Hamilton, T. P.; Shaikh, A. W. *Inorg. Chem.* **1997**, *36*, 754−755.

(27) Davy, R. D.; Schaefer, H. F., III. *Inorg. Chem.* **1998**, *37*, 2291−2295.

(28) Fink, W. H.; Power, P. P.; Allen, T. L. *Inorg. Chem.* **1997**, *36*, 1431−1436.

(29) Brothers, P. J.; Power, P. P. *Adv. Organomet. Chem.* **1996**, *39*, 1−69. Power, P. P. *Chem. Rev.* **1999**, *99*, 3463−3503.

(30) Himmel, H.-J.; Downs, A. J.; Greene, T. M. *J. Chem. Soc., Chem. Commun.* **2000**, 871−872.

Experimental Section

Aluminum (Aldrich, purity 99.999%), gallium (Aldrich, purity 99.9999%), and indium (Aldrich, purity 99.999%) were each evaporated from a tantalum Knudsen cell that was heated resistively, to ca. 1000 °C for Al and 900 °C for Ga and In. Hence the metal vapor was co-deposited with an excess of NH_3-doped argon on a CsI window cooled normally to ca. 12 K by means of a Displex closed-cycle refrigerator (Air Products model CS202). Fuller details of the matrix apparatus are given elsewhere.[14] The estimated proportions M:NH_3:Ar (M = Al, Ga, or In) were typically in the order 1:2−12:600. Typical deposition rates were ca. 2 mmol of matrix gas per hour, continued over a period of 2−3 h. Similar experiments were carried out with ND_3 or $^{15}NH_3$ in place of NH_3. In some experiments too the argon matrix gas was doped not only with ammonia but also with up to 5% of H_2 or D_2.

The following materials were used as received from the sources and with the stated purities listed: NH_3 (Aldrich, >99.99%), ND_3 (Aldrich, 99 at. % D), $^{15}NH_3$ (Aldrich, 98 at. % ^{15}N), H_2 (BOC, Research grade), D_2 (Aldrich, 99.98 at. %), and argon (BOC, Research grade). Gas mixtures of argon with ammonia or with ammonia and dihydrogen were prepared by standard manometric methods.

Following deposition and IR or UV−vis analysis of the resulting matrix, the sample was exposed first to UV radiation with $\lambda = 200-400$ nm or to visible radiation with $\lambda =$ ca. 436 nm. Once the effects of such photolysis had been assessed, the sample was typically irradiated with broad-band UV−visible light with $\lambda = 200-800$ nm. The photolyzing radiation issuing from a Spectral Energy Hg−Xe arc lamp operating at 800 W was invariably limited by a water filter to absorb infrared radiation and so minimize any heating effects. UV light with $\lambda = 200-400$ nm was provided by the use of a visible block filter (Oriel). Visible radiation with $\lambda =$ ca. 436 nm and a band-pass of 20 nm was delivered via an appropriate interference filter (Oriel).

IR spectra of the matrix samples were recorded, typically at a resolution of 0.5 cm^{-1} and with an accuracy of ±0.1 cm^{-1}, using a Nicolet Magna-IR 560 FTIR spectrometer equipped with a liquid N_2-cooled MCTB or with a DTGS detector (for the ranges 4000−400 or 600−200 cm^{-1}, respectively). UV−vis spectra were recorded in the range 300−900 nm using a Perkin-Elmer-Hitachi model 330 spectrophotometer.

Density functional theory (DFT) calculations were performed using the GAUSSIAN 98 program package[31] and applying the B3LYP method, which has been shown to give satisfactory results for small aluminum and gallium compounds.[32] A 6-311G(d) basis set was used for Al and Ga, a LANL2DZ basis set with additional d-polarization functions (exponent 0.5) for In.

Results

The IR spectra associated with the products of the matrix reactions with ammonia will be reported in turn for aluminum, gallium, and indium atoms, respectively. Bands have been assigned on the basis of the following criteria: (i) their growth and decay characteristics in response to photolysis of the matrix under different conditions or to changes of reagent concentration; (ii) comparisons with the results of control experiments that did not include the metal atoms, or with the spectra of related species; (iii) consideration of the selection rules expected to govern the IR activity of a given molecule; (iv) the observed effects of the naturally occurring ^{69}Ga and ^{71}Ga isotopes and of D- or ^{15}N-enrichment of the ammonia precursor; and (v) collation of the measured spectroscopic properties with those forecast by DFT calculations. Additionally, the UV−vis spectra of the matrices afforded a means of tracing the fate of the metal atoms through their interaction with ammonia molecules and the reactions subsequently induced by photolysis.

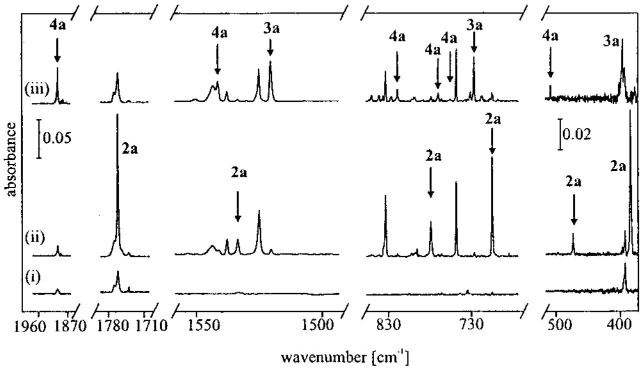

Figure 1. IR spectra of an Ar matrix containing Al and NH_3: (i) following deposition, (ii) following UV photolysis ($\lambda = 200-400$ nm), and (iii) following broad-band UV−visible photolysis ($\lambda = 200-800$ nm).

Aluminum. (a) IR Spectra. The spectrum recorded after deposition of Al together with 2% NH_3 in an argon matrix showed, besides the absorptions of NH_3 and $[NH_3]_n$,[33] three new absorptions at 3447.1, 1593.6, and 1131.4 cm^{-1} due to a first reaction product **1a**. The only other features in the spectrum, invariably weak, were those associated with traces of impurity (H_2O, $[H_2O]_n$, CO_2, and CO)[34] that could be reduced to a minimum but never wholly eliminated. As reported previously,[35] the H_2O gave rise to the insertion product HAlOH, which could be identified by its characteristic absorption at 1739.6 cm^{-1}.

Upon photolysis at wavelengths near 436 nm or with UV light ($\lambda = 200-400$ nm) for a period of 5 min, the signals due to **1a** were extinguished and new signals at 3476.4, 1761.1, 1533.6, 778.7, 705.2, 483.8, 482.2, and 393.8 cm^{-1} were observed to develop [see Figure 1(ii)]. According to their response to different photolysis times and to changes in the NH_3 or Al concentrations, these signals were judged to belong to a common absorber **2a**. The intense absorption at 1761.1 cm^{-1} is close to the Al−H stretching frequencies observed in Al(II) species (e.g., AlH_2 1806.3/1769.5,[10] HAlOH 1739.6,[35] CH_3AlH 1764/1746 cm^{-1} [11]). In addition, the spectrum witnessed the appearance of three bands at 1525.1, 833.4, and 748.2 cm^{-1}. These signals were found to decrease in experiments in which the concentration of NH_3 was reduced to 0.2%. The most likely explanation is that the signals belong to an ammonia adduct of **2a**.

After further photolysis, but with broad-band UV−visible radiation ($200 \leq \lambda \leq 800$ nm), the signals due to **2a** were found to decay with the simultaneous appearance and growth of a new family of bands located at 3495.1, 1520.3, 726.5, and 406.5 cm^{-1} and belonging to a single carrier **3a** [see Figure 1(iii)]. Rather slower to develop but becoming increasingly conspicuous on continued photolysis was a second family of bands located at 3499.7, 1899.3, 1891.0, 1541.6, 818.7, 769.8, 755.0, 608.7, and 518.3 cm^{-1} [see Figure 1(iii)], those at 1899.3, 818.7, 769.8,

---

[31] Frisch, M. J.; Trucks, G. W.; Schlegel, H. B.; Scuseria, G. E.; Robb, M. A.; Cheeseman, J. R.; Zakrzewski, V. G.; Montgomery, J. A., Jr.; Stratmann, R. E.; Burant, J. C.; Dapprich, S.; Millam, J. M.; Daniels, A. D.; Kudin, K. N.; Strain, M. C.; Farkas, O.; Tomasi, J.; Barone, V.; Cossi, M.; Cammi, R.; Mennucci, B.; Pomelli, C.; Adamo, C.; Clifford, S.; Ochterski, J.; Petersson, G. A.; Ayala, P. Y.; Cui, Q.; Morokuma, K.; Malick, D. K.; Rabuck, A. D.; Raghavachari, K.; Foresman, J. B.; Cioslowski, J.; Ortiz, J. V.; Stefanov, B. B.; Liu, G.; Liashenko, A.; Piskorz, P.; Komaromi, I.; Gomperts, R.; Martin, R. L.; Fox, D. J.; Keith, T.; Al-Laham, M. A.; Peng, C. Y.; Nanayakkara, A.; Gonzalez, C.; Challacombe, M.; Gill, P. M. W.; Johnson, B.; Chen, W.; Wong, M. W.; Andres, J. L.; Gonzalez, C.; Head-Gordon, M.; Replogle, E. S.; Pople, J. A. *GAUSSIAN 98*, Revision A.3; Gaussian Inc.: Pittsburgh, PA, **1998**.

[32] Jursic, B. S. *J. Mol. Struct.: THEOCHEM* **1998**, *428*, 61−66.

[33] See, for example: Süzer, S.; Andrews, L. *J. Chem. Phys.* **1987**, *87*, 5131−5140. Abouaf-Marguin, L.; Jacox, M. E.; Milligan, D. E. *J. Mol. Spectrosc.* **1977**, *67*, 34−61.

[34] Greene, T. M.; Andrews, L.; Downs, A. J. *J. Am. Chem. Soc.* **1995**, *117*, 8180−8187.

[35] Hauge, R. H.; Kauffman, J. W.; Margrave, J. L. *J. Am. Chem. Soc.* **1980**, *102*, 6005−6011.

Table 1. Infrared Absorptions (Frequencies in cm^{-1}) Displayed by Ar Matrices Containing Al Atoms and $^{14}NH_3$/$^{15}NH_3$/$^{14}ND_3$

Al + $^{14}NH_3$	Al + $^{15}NH_3$	Al + $^{14}ND_3$	deposition[a]	$\lambda = 436$ nm[a]	$\lambda = 200-800$ nm[a]	absorber
3499.7	*b*	*b*			↑	H_2AlNH_2, **4a**
3495.1	3486.2	*b*			↑	$AlNH_2$, **3a**
3476.4	3468.2	2595.6		↑	↓	$HAlNH_2$, **2a**
3447.1	*b*	*b*	↑	↓		$Al{\cdot}NH_3$, **1a**
1899.3	1899.3	1384.2			↑	H_2AlNH_2, **4a**
1891.0	1891.0	*b*			↑	H_2AlNH_2, **4a**
1887.6	1887.4	1364.7			↑	$H_2AlNH_2{\cdot}NH_3$
1761.1	1761.0	1282.6		↑	↓	$HAlNH_2$, **2a**
1593.6	*b*	*b*	↑	↓		$Al{\cdot}NH_3$, **1a**
1590.9	1590.9	*b*			↑	AlH
1541.6	1536.1	1159.5			↑	H_2AlNH_2, **4a**
1533.6	1531.5	1151.4		↑	↓	$HAlNH_2$, **2a**
1525.1	1520.0	1149.5		↑	↓	$HAlNH_2{\cdot}NH_3$
1520.3	1515.0	1137.8			↑	$AlNH_2$, **3a**
1131.4	1125.6	972.6	↑	↓		$Al{\cdot}NH_3$, **1a**
833.4	821.4	*b*		↑	↓	$HAlNH_2{\cdot}NH_3$
818.7	809.8	*b*			↑	H_2AlNH_2, **4a**
778.7	766.9	748.3		↑	↓	$HAlNH_2$, **2a**
769.8	766.2	611.0			↑	H_2AlNH_2, **4a**
755.0	*b*	548.4			↑	H_2AlNH_2, **4a**
748.2	*b*	*b*		↑		$HAlNH_2{\cdot}NH_3$
726.5	713.6	694.9			↑	$AlNH_2$, **3a**
705.2	701.0	549.8		↑	↓	$HAlNH_2$, **2a**
608.7	608.1	450.4			↑	H_2AlNH_2, **4a**
518.3	516.7	397.7			↑	H_2AlNH_2, **4a**
483.8	483.2	346.5		↑	↓	$HAlNH_2$, **2a**
482.2	*b*	*b*		↑	↓	$HAlNH_2$, **2a**
406.5	403.9	314.6			↑	$AlNH_2$, **3a**
393.8	391.9	304.6		↑	↓	$HAlNH_2$, **2a**

[a] ↑, increase; ↓, decrease. [b] Too weak to be detected or hidden by NH_3 absorptions.

and 608.7 cm^{-1} being the most prominent. With constant relative intensities these arose from a common product **4a**. Diagnostic features of the spectrum are (i) the strong absorption at 1899.3 cm^{-1} occurring in the region characteristic of the stretching vibrations of terminal Al(III)−H bonds [cf. AlH_3 (1882.9 cm^{-1}),[10] $HAlCl_2$ (1967.6 cm^{-1}),[36] and $[H_2AlNMe_2]_3$ (1800−1850 cm^{-1})[37]], (ii) the absorptions at 3499.7, 1541.6, and 608.7 cm^{-1}, which are suggestive of the presence of an amido group, NH_2,[38] and (iii) the appearance of an absorption at 818.7 cm^{-1}, which lies within the region expected for a ν(Al−N) mode of an aluminum(III) compound.[19,39] In addition to these signals, a very weak absorption at 1887.6 cm^{-1} was observed.

Experiments in which the matrix concentration of ammonia was reduced from 2 to 0.2%, while the other conditions remained as before, gave results identical to those described above, insofar as the intensities of the bands permitted them to be detected, but with one important difference: the yield of **4a** was reduced quite disproportionately—almost to vanishing point—in relation to those of **2a** and **3a**. In another series of experiments, the matrix was doped not only with 2% NH_3 but also with up to 5% H_2. There was no sign of any reaction on deposition beyond the appearance of the IR bands associated with **1a**. UV photolysis ($200 \leq \lambda \leq 400$ nm) led as before to the formation of **2a** but now in company with AlH_2 (recognizable by the appearance of prominent IR absorptions at 1806.3, 1769.5, and 766.4 cm^{-1}) as the principal photoproduct deriving from the reaction of photoexcited Al atoms with H_2 under these conditions.[10] Irradiation with broad-band UV−visible light ($200 \leq \lambda \leq 800$ nm) then led to the formation of the products **3a** and **4a**, but now with a significantly *higher* yield of **4a** compared with **3a** than in comparable experiments with H_2-free matrices. The signal at 1887.6 cm^{-1} also gained in intensity. As expected,[10] there was a simultaneous decay of the bands due to AlH_2, these being replaced (i) by a single band at 1649.1 cm^{-1} and (ii) by a family of three bands at 1882.9, 783.6, and 697.7 cm^{-1} readily identifiable with the molecules AlH and AlH_3, respectively.

The experiment was repeated successively with ND_3 and $^{15}NH_3$ with the results included in Table 1. The signal at 1131.4 cm^{-1} due to the species **1a** underwent a substantial shift in the experiment employing ND_3 (H/D = 1.1633:1) and a shift of −5.8 cm^{-1} in that with $^{15}NH_3$.

The signals of product **2a** at 3476.4 and 1533.6 cm^{-1} exhibited H/D ratios of 1.3393:1 and 1.3319:1 and ^{15}N shifts of −8.2 and −2.1 cm^{-1}, whereas the 1761.1 cm^{-1} signal showed an H/D ratio of 1.3731:1 and almost no ^{15}N shift, in agreement with its assignment to an Al−H stretching fundamental. The bands at 705.2, 483.8, and 393.8 cm^{-1} exhibited H/D ratios of 1.2826:1, 1.3962:1, and 1.2928:1 and ^{15}N shifts of −4.2, −0.6 and −1.9 cm^{-1}, respectively. No counterpart to the weak feature at 482.2 cm^{-1} could be discerned in the $^{15}NH_3$ or ND_3 experiments, being either too weak to be observed or hidden by other, stronger absorptions.

All four IR signals associated with the product **3a** could be traced to analogous features in the experiments with $^{15}NH_3$ and ND_3. In keeping with its attribution to the scissoring fundamental of an NH_2 fragment, the absorption at 1520.3 cm^{-1} exhibited an H/D ratio of 1.3362:1 and a ^{15}N shift of −5.3 cm^{-1}. The presence of an NH_2 unit is also suggested by the band at 3495.1 cm^{-1} with a ^{15}N shift of −8.9 cm^{-1}. The bands at 726.5 and 406.5 cm^{-1} were characterized by H/D ratios of 1.0455:1 and 1.2921:1, and ^{15}N shifts of −2.9 and −2.6 cm^{-1}, respectively.

---

(36) Schnöckel, H. *J. Mol. Struct.* **1978**, *50*, 275−280.

(37) Downs, A. J.; Duckworth, D.; Machell, J. C.; Pulham, C. R. *Polyhedron* **1992**, *11*, 1295−1304.

(38) Nakamoto, K. *Infrared and Raman Spectra of Inorganic and Coordination Compounds*, 5th ed.; Wiley-Interscience: New York, 1997; Part B. Lappert, M. F.; Power, P. P.; Sanger, A. R.; Srivastava, R. C. *Metal and Metalloid Amides*; Ellis Horwood: Chichester, U.K., 1980.

(39) Müller, J. *J. Am. Chem. Soc.* **1996**, *118*, 6370−6376.

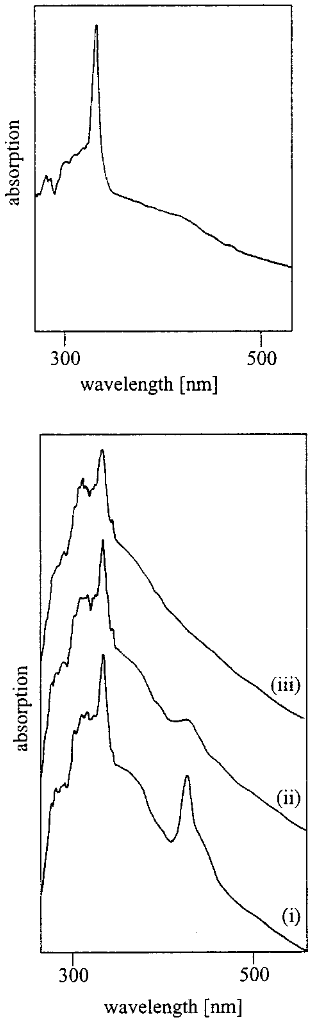

Figure 2. UV−vis spectra (a, top) of an Ar matrix containing Al, and (b, bottom) of an Ar matrix containing Al and NH_3: (i) following deposition, (ii) following photolysis with radiation having $\lambda = 436$ nm, and (iii) following broad-band UV−visible photolysis ($\lambda = 200-800$ nm).

The strong band at 1899.3 cm^{-1} of product **4a** exhibited a large frequency shift on deuteration (H/D = 1.3721:1), but no significant ^{15}N shift. Deuteration also elicited substantial shifts on the part of the bands at 1541.6 (H/D = 1.3295:1), 769.8 (H/D = 1.3010:1), 755.0 (1.3767:1), 608.7 (1.3515:1), and 518.3 cm^{-1} (1.3032:1), while ^{15}N shifts amounting to −5.5, −3.6, −0.6, and −1.6 cm^{-1} were registered by the bands at 1541.6, 769.8, 608.7, and 518.3 cm^{-1}, respectively. The largest ^{15}N shift (−8.9 cm^{-1}) was associated with the feature at 818.7 cm^{-1} for which it was unfortunately impossible to locate a counterpart in the ND_3 experiments, presumably because of the masking effects of other absorptions.

(b) UV−Vis Spectra. Figure 2 depicts the UV−vis spectra measured over the range 300−900 nm for aluminum vapor isolated (a) in a pure argon matrix and (b) in an argon matrix doped with 2% NH_3. The first spectrum featured a strong absorption at 337 nm, which can be assigned on the basis of earlier studies[40] to the $^2S \leftarrow {}^2P$ transition of Al atoms. When the matrix included NH_3, this was accompanied by a new absorption at 428 nm. Irradiation of the NH_3-doped matrix for 5 min at wavelengths near 436 nm led to the disappearance of the new band. The IR spectrum measured at this stage witnessed the disappearance of the bands associated with **1a** as well as an increase of those due to the photoproduct **2a**.

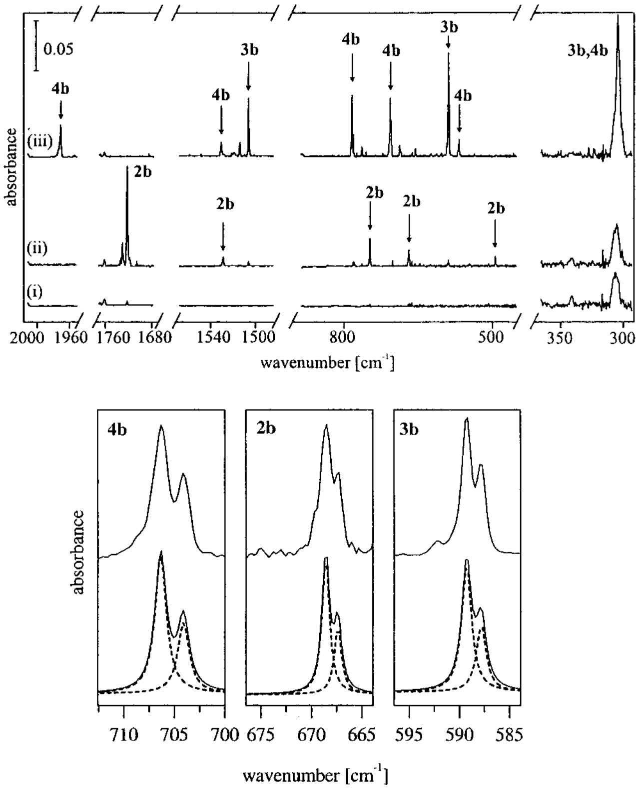

Figure 3. IR spectra of an Ar matrix containing Ga and NH_3: (a, top) (i) following deposition, (ii) following UV photolysis ($\lambda = 200-400$ nm), and (iii) following broad-band UV−visible photolysis ($\lambda = 200-800$ nm); (b, bottom) bands near 700 (**4b**), 670 (**2b**), and 590 cm^{-1} (**3b**) showing $^{69}Ga/^{71}Ga$ splitting.

Gallium. (a) IR Spectra. Figure 3 depicts the IR spectra displayed by an argon matrix containing ca. 0.2% Ga atoms and 2% NH_3 before and after photolysis; details of the spectra are itemized in Table 2. On deposition, the matrix exhibited in addition to the absorptions characteristic of NH_3 and $[NH_3]_n$[33] new features at 3441.5, 1580.7, and 1104.2 cm^{-1} carried by a common product **1b**. The only other features in the spectrum arose from traces of impurity (H_2O, $[H_2O]_n$, CO_2, and CO)[34] including the complex $Ga{\cdot}H_2O$ identifiable by its characteristic absorption at 1576.1 cm^{-1}.[35]

Exposure of the matrix to radiation at λ = ca. 436 nm or to UV radiation ($\lambda = 200-400$ nm) for 5 min brought about significant changes, as revealed by the IR spectrum measured at this stage [Figure 3a(ii)]. The bands due to **1b** had disappeared to be replaced by new ones at 1721.8, 1528.7, 746.2, 668.5/667.4, 494.1, and 210.9 cm^{-1} all attributable on the strength of their constant relative intensities to a second product **2b**. The most intense and distinctive features were those at 1721.8, 668.5/667.4, and 210.9 cm^{-1}, of which the first comes close in frequency to the Ga−H stretching fundamentals of the gallium(II) species GaH_2 (1799.5/1727.7 cm^{-1}),[10] CH_3GaH (1719.7 cm^{-1}),[14] and HGaOH (1669.8 cm^{-1}).[35] The partially resolved doublet pattern at 668.5/667.4 cm^{-1} revealed components with relative intensities of ca. 1.5:1 suggesting that it originates in a vibration involving appreciable motion of a single Ga atom (^{69}Ga and ^{71}Ga in natural Ga being in the proportion 1.507:1[41]). Continued irradiation under these conditions produced little further change in the spectrum.

---

(40) Ammeter, J. H.; Schlosnagle, D. C. *J. Chem. Phys.* **1973**, *59*, 4784−4820.

(41) Lide, D. R., Editor-in-Chief. *CRC Handbook of Chemistry and Physics*, 80th ed.; CRC Press: Boca Raton, FL, 1999−2000.

Table 2. Infrared Absorptions (Frequencies in cm^{-1}) Displayed by Ar Matrices Containing Ga Atoms and $^{14}NH_3$/$^{15}NH_3$/$^{14}ND_3$

Ga + $^{14}NH_3$	Ga + $^{15}NH_3$	Ga + $^{14}ND_3$	deposition[a]	$\lambda = 436$ nm[a]	$\lambda = 200-800$ nm[a]	absorber
3510.7	3500.7	*b*			↑	H_2GaNH_2, **4b**
b	3485.4	*b*		↑	↓	$HGaNH_2$, **2b**
3471.6	*b*	*b*			↑	$GaNH_2$, **3b**
3441.5	*b*	*b*	↑	↓		$Ga{\cdot}NH_3$, **1b**
3413.4	3405.9	*b*			↑	H_2GaNH_2, **4b**
1970.8[c]	1970.7[c]	1419.1			↑	H_2GaNH_2, **4b**
1970.8[c]	1970.7[c]	1407.7			↑	H_2GaNH_2, **4b**
1942.0	1942.0	*b*			↑	$H_2GaNH_2{\cdot}NH_3$
1721.8	1721.8	1249.5		↑	↓	$HGaNH_2$, **2b**
1580.7	1576.9	*b*	↑	↓		$Ga{\cdot}NH_3$, **1b**
1530.4	1524.3	1150.9			↑	H_2GaNH_2, **4b**
1528.7	1523.2	1145.0		↑	↓	$HGaNH_2$, **2b**
1513.8	1513.8	1090.1			↑	GaH
1505.9	1501.2	1132.6			↑	$GaNH_2$, **3b**
1104.2	1099.1	824.9	↑	↓		$Ga{\cdot}NH_3$, **1b**
782.8	778.3	605.1			↑	H_2GaNH_2, **4b**
779.6	775.2	568.8			↑	H_2GaNH_2, **4b**
754.3	751.0	*b*			↑	$H_2GaNH_2{\cdot}NH_3$
746.2	743.7	563.5		↑	↓	$HGaNH_2$, **2b**
706.2/704.1	692.2/690.0	667.8/665. 2			↑	H_2GaNH_2, **4b**
668.5/667.4	652.8/651.4	626.8/625. 1		↑	↓	$HGaNH_2$, **2b**
589.3/587.9	574.3/573.1	557.9/556. 4			↑	$GaNH_2$, **3b**
567.7	567.4	405.9			↑	H_2GaNH_2, **4b**
494.1	494.1	*b*		↑	↓	$HGaNH_2$, **2b**
304.9	302.8	*b*			↑	H_2GaNH_2, **4b**
303.3	302.7	*b*			↑	$GaNH_2$, **3b**
210.9	*b*	*b*		↑	↓	$HGaNH_2$, **2b**

[a] ↑, increase; ↓, decrease. [b] Too weak to be detected or hidden by NH_3 absorptions. [c] Two modes contained within a single broad absorption.

By contrast, after photolysis for a further 30 min, but with broad-band UV−visible light ($200 \le \lambda \le 800$ nm), the matrix gave the IR spectrum illustrated in Figure 3a(iii). Hence it is apparent that the absorptions due to **2b** have decayed, while a new family of absorptions having a common origin in a third product **3b** has simultaneously appeared. These occurred at 3471.6, 1505.9, 589.3/587.9, and 303.3 cm^{-1}, with the last two features being the most intense, and the doublet structure of the penultimate feature having all the hallmarks of $^{69}Ga/^{71}Ga$ isotopic splitting. Extending the period of photolysis led to the buildup of **3b** at the expense of **2b**.

In addition to the bands due to **3b**, another family of bands, also with constant relative intensities and therefore originating in a fourth distinct product **4b**, was observed to develop [see Figure 3a(iii)], becoming increasingly prominent with photolysis times exceeding 30 min. The members of this family were located at 3510.7, 3413.4, 1970.8, 1530.4, 782.8, 779.6, 706.2/704.1, 567.7, and 304.9 cm^{-1}, those at 1970.8, 782.8, 706.2/704.1, and 304.9 cm^{-1} being the most intense (see Table 2). As in the case of the corresponding aluminum compound **4a**, there are several clues to the identity of **4b**: (i) the absorptions at 1970.8 and 779.6 cm^{-1} are strongly suggestive of a terminal GaH_2 unit in a trivalent gallane derivative [cf. GaH_3 (1923.2 and 758.7 cm^{-1}),[10] H_2GaCl (1964.6/1978.1 and 731.4 cm^{-1}),[42] $H_2Ga(\mu\text{-}Cl)_2GaH_2$ (1994/2036 and 702/719 cm^{-1}),[43] and $H_2Ga(\mu\text{-}H)_2BH_2$ (1982/2005 and 729 cm^{-1})[44]]; (ii) the absorptions at 3510.7, 3413.4, 1530.4, 782.8, and 567.7 cm^{-1} bear all the hallmarks of an NH_2 group; and (iii) the doublet pattern at 706.2/704.1 cm^{-1} implies $^{69}Ga/^{71}Ga$ splitting arising from the motion of a single Ga atom, possibly in a ν(Ga−N) vibration. Once all signs of **2b** had disappeared, continued photolysis evoked little further change in the spectrum, **3b** and **4b** being the ultimate photoproducts. In addition, the IR spectra contained very weak signals at 1942.0 and 754.3 cm^{-1}, which developed simultaneously with those due to **4b**.

Experiments in which the matrix concentration of ammonia was reduced from 2 to 0.2%, while the other conditions remained as before, gave results identical to those described above, insofar as the intensities of the bands permitted them to be detected, but with one important difference: the yield of **4b** was reduced much more markedly than those of **2b** and **3b**.

In another series of experiments the matrix was doped not only with 2% NH_3 but also with up to 5% H_2. The only signs of any reaction on deposition, beyond the appearance of the IR bands associated with **1b**, were those noted previously[12,16] and by us[17] for matrices formed by quenching Ga vapors with H_2 and pointing to the spontaneous reaction of Ga_2 dimers with H_2 to give $Ga(\mu\text{-}H)_2Ga$. UV photolysis led, as before, to the formation of **2b** but now in company with GaH_2 (recognizable by the appearance of prominent IR absorptions at 1799.5, 1727.7, and 740.1 cm^{-1}) as the principal photoproduct deriving from the reaction of photoexcited Ga with H_2 under these conditions.[10,12] Irradiation with broad-band UV−visible light then led to the formation of the products **3b** and **4b**, but now with a significantly *higher* yield of **4b** than in comparable experiments with H_2-free matrices. As expected, there was a simultaneous decay of the bands due to GaH_2, these being replaced by a single band at 1571.3 cm^{-1} readily identifiable with the diatomic GaH molecule.[10,12]

To gain more information about the species **1b**−**4b**, the experiments were repeated using either ND_3 or $^{15}NH_3$ as the reagent, with the results included in Table 1. Hence it appeared that the perdeuterated version of the feature at 1104.2 cm^{-1} due to **1b** was characterized by an IR band at 824.9 cm^{-1}, whereas the $^{15}NH_3$ version revealed a ^{15}N shift of −5.1 cm^{-1}. The signal at 1580.7 cm^{-1} exhibited a ^{15}N shift of −3.8 cm^{-1}.

All the IR features of **2b** that could be observed with the switch from NH_3 to ND_3 appeared at lower frequency. Thus the bands at 1721.8, 1528.7, 746.2, and 668.5/667.4 cm^{-1} for

---

(42) Köppe, R.; Schnöckel, H. *J. Chem. Soc., Dalton Trans.* **1992**, 3393−3395.

(43) Johnsen, E.; Downs, A. J.; Greene, T. M.; Souter, P. F.; Aarset, K.; Page, E. M.; Rice, D. A.; Richardson, A. N.; Brain, P. T.; Rankin, D. W. H.; Pulham, C. R. *Inorg. Chem.* **2000**, *39*, 719−727.

(44) Pulham, C. R. D. Philos. Thesis, University of Oxford, U.K., 1991.

the natural isotopomer shifted to 1249.5 (H/D = 1.3780:1), 1145.0 (H/D = 1.3351:1), 563.5 (H/D = 1.3242:1), and 626.8/625.1 cm^{-1} (H/D = 1.0665:1, 1.0677:1), respectively. No counterparts to the weak band at 494.1 cm^{-1} and the stronger one at 210.9 cm^{-1} could be observed for the perdeuterated version of **2b**, being either too weak to be detected or obscured by absorption from another source in the first case or outside the lower limit of detection (200 cm^{-1}) in the second case. The IR spectrum of the ^{15}N isotopomer of **2b** resembled closely that of the natural form; while it lacked a band near 200 cm^{-1} correlating with the lowest frequency transition of the latter, it included an additional band at 3485.4 cm^{-1} strongly suggestive of a ν(N−H) mode. Of the bands in the spectrum of the natural isotopomer only those at 1528.7, 746.2, and 668.5/667.4 cm^{-1} experienced significant frequency changes (−5.5, −2.5, and −15.7 to −16.0 cm^{-1}, respectively) on ^{15}N substitution.

Three of the four absorptions associated with **3b** found parallels in the measured spectra of the perdeuterated and ^{15}N isotopomers. For example, those at 1505.9 and 589.3/587.9 cm^{-1} moved to 1132.6 (H/D = 1.3296:1) and 557.9/556.4 cm^{-1} (H/D = 1.0563:1, 1.0566:1), respectively, on deuteration, and showed $^{14}N/^{15}N$ shifts (of −4.7 and −14.9 cm^{-1}). No analogue of the weak band at 3471.6 cm^{-1} associated with the isotopically normal form of **3b** could be discerned for either the deuterated or ^{15}N version, presumably for want of intensity and/or because of the masking effects of the more intense bands due to monomeric or oligomeric ammonia molecules.[33]

In its perdeuterated guise **4b** was characterized by eight detectable IR-active transitions. Hence the following shifts were observed: 1970.8 to 1419.1 cm^{-1} (H/D = 1.3888:1), 1970.8 to 1407.7 cm^{-1} (H/D = 1.4000:1), 1530.4 to 1150.9 cm^{-1} (H/D = 1.3297:1), 782.8 to 605.1 cm^{-1} (H/D = 1.2937:1), 779.6 to 568.8 cm^{-1} (H/D = 1.3706:1), 706.2/704.1 to 667.8/665.2 cm^{-1} (H/D = 1.058:1), and 567.7 to 405.9 cm^{-1} (H:D = 1.3986:1). It was not possible to locate any bands in the spectrum of the deuterated compound corresponding to those at 3510.7, 3413.4, and 304.9 cm^{-1} due to the isotopically natural species. ^{15}N substitution resulted in significant $^{14}N/^{15}N$ shifts on the part of the features at the following frequencies (in cm^{-1}): 3510.7 (−10.0), 3413.4 (−7.5), 1530.4 (−6.1), 782.8 (−4.5), 779.6 (−4.4), 706.2/704.1 (−14.0), and 304.9 (−2.1). By contrast, there was little or no change in the frequencies of the intense band at 1970.8 cm^{-1} or the weaker one at 567.7 cm^{-1}.

Experiments were also carried out with matrices containing Ga atoms and both NH_3 and D_2. The presence of D_2 had no effect on the IR spectra characterizing the molecules **1b**, **2b**, and **3b**, which betrayed no sign of H/D exchange. On the other hand, the spectrum of **4b** was made distinctly more complicated, arguing for the presence of both Ga−H and Ga−D bonds in different H/D isotopomers of the molecule. As will be shown, these findings are highly germane in the mechanistic implications they carry.

(b) UV−Vis Spectra. Figure 4 shows typical UV−vis spectra measured over the range 300−900 nm for gallium vapor isolated (a) in a pure argon matrix and (b) in an argon matrix doped with 2% NH_3. The furnace temperature for the evaporation of the gallium was set relatively low (ca. 900 °C) in this and all the other experiments so that Ga atoms should be the predominant metal species trapped in the matrices, with a negligible involvement of oligomers such as Ga_2. Following deposition, the NH_3-doped matrix was found to exhibit two prominent absorptions, one at 345 nm and the other at 440 nm. The former is recognizable on the basis of earlier studies[13,14] as the $^2S \leftarrow {}^2P$ transition of Ga atoms isolated in an argon matrix cage. The latter must then be associated with a relatively specific interaction between the Ga atoms and NH_3 dopant molecules, possibly corresponding to what is essentially a metal-based $^2S \leftarrow {}^2P$ transition in a complex of the type $Ga(NH_3)_n$.

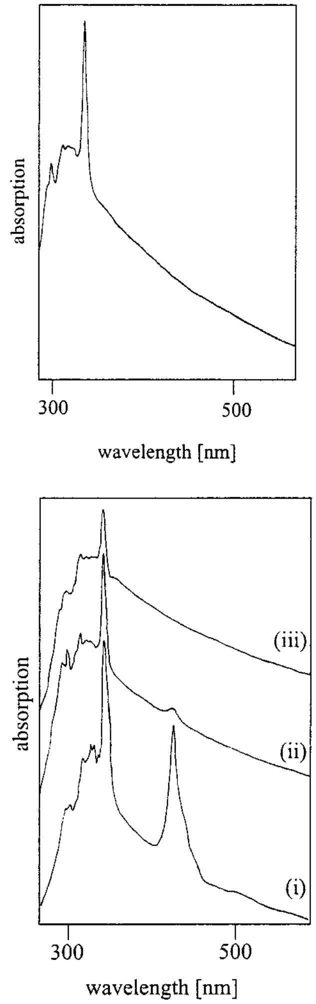

Figure 4. UV−vis spectra (a, top) of an Ar matrix containing Ga, and (b, bottom) of an Ar matrix containing Ga and NH_3: (i) following deposition, (ii) following photolysis with radiation having $\lambda = 436$ nm, and (iii) following broad-band UV−visible photolysis ($\lambda = 200-800$ nm).

After 10 min irradiation with UV light ($\lambda = 200-400$ nm) or with visible light having $\lambda =$ ca. 436 nm, it was found that the absorption at 440 nm had been virtually extinguished. The IR spectrum of the matrix measured at this stage witnessed the disappearance of the bands due to **1b** as well as the emergence of those due to the product **2b**. The UV absorption at 345 nm had also decayed somewhat but to a smaller extent. No new absorption could be detected either at this juncture or after exposure of the matrix to broad-band UV−visible radiation ($\lambda = 200-800$ nm), the only perceptible change in the UV−vis spectrum then being a further decrease in the intensity of the 345 nm signal. The IR measurements serve therefore to confirm that the initial appearance of the product **2b** is linked not only to the decay of the IR bands attributed to **1b** but also to that of the 440 nm band, providing strong circumstantial grounds for believing that **1b** is also the author of this latter feature.

Indium. (a) IR Spectra. Experiments with ammonia-doped argon matrices including indium in place of gallium followed

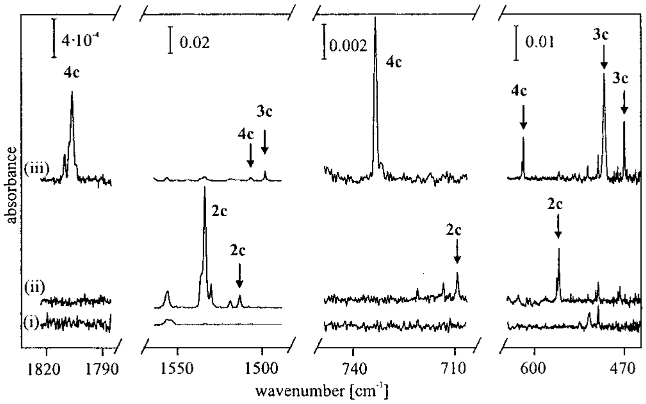

Figure 5. IR spectra of an Ar matrix containing In and NH_3: (i) following deposition, (ii) following UV photolysis ($\lambda = 200-400$ nm), and (iii) following broad-band UV−visible photolysis ($\lambda = 200-800$ nm).

the same pattern as those described above, and led to the identification of four products **1c**, **2c**, **3c**, and **4c** clearly analogous to the corresponding aluminum- and gallium-containing products **1a**−**4a** and **1b**−**4b**. A set of representative IR spectra measured for an argon matrix containing ca. 0.2% In atoms and 2% NH_3 is reproduced in Figure 5; the relevant details of the spectra are listed in Table 3. Following deposition the spectrum [Figure 5(i)] witnessed the appearance of new absorptions at 3424.4 and 1082.9 cm^{-1} requiring the conjunction of In and NH_3 and attributable on the evidence of the earlier experiments to a complex **1c**, i.e., the In analogue of **1a** and **1b**. The only other features of the spectrum at this stage could be attributed to unchanged NH_3 or $[NH_3]_n$[33] or to traces of the inevitable impurities, including H_2O, $[H_2O]_n$, the adduct $In{\cdot}H_2O$, CO_2, etc.[34,35]

Irradiation of the matrix at $\lambda =$ ca. 436 or 200−400 nm for 5 min resulted in the decay of the absorptions due to **1c** and the growth of five new absorptions at 3463.5, 1533.8, 1512.9, 709.0, and 564.8 cm^{-1} having but a single carrier, as indicated in Figure 5(ii). The most intense and distinctive feature was the one near 1530 cm^{-1}, which occurs in the region where the In−H stretching mode of an indium(II) hydride might be expected (cf. 1615.6/1548.6, 1545.9, and 1486.5 cm^{-1} for InH_2,[10] CH_3InH,[14] and HInOH,[35] respectively). This factor, allied to the obvious affinities to the IR spectra of **2a** and **2b**, leads us to believe that the new bands are most plausibly ascribed to the indium analogue **2c**.

On the other hand, subsequent exposure of the matrix to broad-band UV−visible radiation ($\lambda = 200-800$ nm) for 30 min brought about the decay of the bands due to **2c** with simultaneous growth of a new family of absorptions at 3481.7, 1498.1, 498.7, 469.6, and 237.0 cm^{-1}. Given the circumstances of the experiment, the spectroscopic resemblance of this third product to **3a** and **3b** affords persuasive evidence that it is to be identified with the indium analogue **3c**. Moreover, weak features first detected at this stage and attributable to a fourth product were observed to grow on continued UV−visible photolysis. Most conspicuous of these was a band at 1805.9 cm^{-1}, a frequency diagnostic of a ν(In−H) mode of an indium(III) hydride (cf. 1754.5, 1820.3/1804.0, and 1846.9 cm^{-1} for InH_3,[10] H_2InCl,[15] and $HInCl_2$,[15] respectively). Other, weaker features associated with this product occurred at 733.3 and 616.3 cm^{-1}. All the signs are consistent therefore with the identification of the product with **4c**, the In counterpart to **4a** and **4b**.

The experiments giving rise to the species **1c**−**4c** were repeated using either ND_3 or $^{15}NH_3$ as the reagent, with the results included in Table 3. Notable aspects of **1c** were the substantial deuterium shift (H/D = 1.3271:1) and small ^{15}N shift (−5.2 cm^{-1}) of the band at 1082.9 cm^{-1} as well as the ^{15}N shift of −11.4 cm^{-1} for the band at 3424.4 cm^{-1}. Four of the features associated with **2c** suffered deuterium shifts with H/D ratios ranging from 1.3833:1 (at 1533.8 cm^{-1}) to 1.0681:1 (at 564.8 cm^{-1}). The corresponding ^{15}N shifts were 0 and −13.1 cm^{-1}. Experiments with ND_3 yielded two absorptions identifiable with perdeuterated **3c** (at 1116.3 and 480.6 cm^{-1}) appearing to correlate with the absorptions at 1498.1 and 498.7 cm^{-1} in the spectrum of the normal isotopomer. The H/D ratios were therefore 1.3420:1 and 1.0377:1, respectively. Three features could be definitely traced to the ^{15}N isotopomer indicating ^{15}N shifts amounting to −4.5, −10.5, and −1.6 cm^{-1} for the transitions occurring at 1498.1, 498.7, and 237.0 cm^{-1}, respectively.

Weakness and the potential for masking by the signals due to other, more abundant molecules (NH_3, $[NH_3]_n$, **3c**, etc.) meant that there was only limited access to the IR-active transitions carried by **4c** in its normal, deuterated, or ^{15}N versions. However, decreasing the NH_3 concentration did appear to reduce the yield of **4c** significantly more than that of **3c**, whereas adding H_2 to the matrix boosted the proportion of **4c** relative to **3c**. It was also possible to establish that the 1805.9 cm^{-1} transition moved to 1299.0 cm^{-1} on deuteration of **4c** giving H/D = 1.3902:1 but was unmoved when ^{14}N was replaced by ^{15}N. On the other hand, the bands at 733.3 and 616.3 cm^{-1} displayed ^{15}N shifts of −1.9 and −17.1 cm^{-1}, respectively. With ND_3 as the reagent, a weak band was observed at 474.6 cm^{-1}; this showed the growth pattern characteristic of the IR features belonging to **4c** but could not be traced to any obvious counterparts in the spectra of the normal and ^{15}N versions of the molecule. The yield of **4c** was invariably small; in no case did it match those of its aluminum and gallium analogues. This may reflect significant photolability on its part or lower yields of the intermediates leading to its formation. Although spectroscopic details about **4c** are therefore rather sparse, all the features that could be observed are consistent with the circumstantial evidence pointing to a product akin to **4a** and **4b**.

(b) UV−Vis Spectra. UV−vis spectra of indium vapor entrapped (a) in a pure argon matrix and (b) in an argon matrix doped with 2% NH_3 are depicted in Figure 6. Both spectra include a prominent absorption at 335 nm attributable to the $^2S \leftarrow {}^2P$ transition of In atoms trapped in an argon matrix cage.[14,45] The presence of NH_3 gave rise, however, to a new intense absorption centered at 435 nm. Irradiation of the matrix with visible light having $\lambda = 436$ nm for 10 min virtually extinguished this second feature. At the same time the IR spectra bore witness to the disappearance of the bands characteristic of **1c** and to the appearance of those characteristic of **2c**. Accordingly we are led to conclude that the visible absorption at 435 nm belongs to **1c** and that irradiation into it offers a highly efficient means of converting **1c** into **2c**. Further photolysis with either broad-band UV or UV−visible light resulted in no change in the UV−vis spectrum of the NH_3-doped matrix beyond the gradual decay of the 335 nm absorption.

Discussion

The main IR features observed to develop as the result of the reactions induced thermally or photolytically on deposition of Al, Ga, or In atoms in an ammonia-doped argon matrix will

---

(45) Schroeder, W.; Rotermund, H.-H.; Wiggenhauser, H.; Schrittenlacher, W.; Hormes, J.; Krebs, W.; Laaser, W. *Chem. Phys.* **1986**, *104*, 435−448.

Table 3. Infrared Absorptions (Frequencies in cm^{-1}) Displayed by Ar Matrices Containing In Atoms and $^{14}NH_3$/$^{15}NH_3$/$^{14}ND_3$

In + $^{14}NH_3$	In + $^{15}NH_3$	In + $^{14}ND_3$	deposition[a]	$\lambda = 436$ nm[a]	$\lambda = 200-800$ nm[a]	absorber
3481.7	*b*	*b*			↑	$InNH_2$, **3c**
3463.5	*b*	*b*		↑	↓	$HInNH_2$, **2c**
3424.4	3413.0	*b*	↑	↓		$In{\cdot}NH_3$, **1c**
1805.9	1805.9	1299.0			↑	H_2InNH_2, **4c**
1533.8	1533.8	1108.8		↑	↓	$HInNH_2$, **2c**
1512.9	*b*	1122.2		↑	↓	$HInNH_2$, **2c**
1506.6	*b*	*b*			↑	H_2InNH_2, **4c**
1498.1	1493.6	1116.3			↑	$InNH_2$, **3c**
1387.3	1387.3	995.8			↑	InH
1082.9	1077.7	816.0	↑	↓		$In{\cdot}NH_3$, **1c**
733.3	731.4	*b*			↑	H_2InNH_2, **4c**
713.3	*b*	*b*		↑	↓	HInOH
709.0	*b*	522.9		↑	↓	$HInNH_2$, **2c**
616.3	599.2	*b*			↑	H_2InNH_2, **4c**
564.8	551.7	528.8		↑	↓	$HInNH_2$, **2c**
522.6	522.6	505.3			↑	InOH
498.7	488.2	480.6			↑	$InNH_2$, **3c**
b	*b*	474.6			↑	H_2InNH_2, **4c**
469.6	*b*	*b*			↑	$InNH_2$, **3c**
237.0	235.4	*b*			↑	$InNH_2$, **3c**

[a] ↑, increase; ↓, decrease. [b] Too weak to be detected or hidden by NH_3 absorptions.

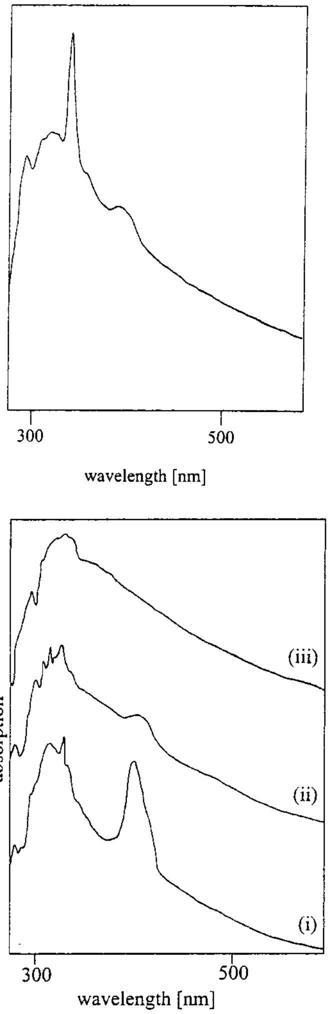

Figure 6. UV−vis spectra (a, top) of an Ar matrix containing In, and (b, bottom) of an Ar matrix containing In and NH_3: (i) following deposition, (ii) following photolysis with radiation having $\lambda = 436$ nm, and (iii) following broad-band UV−visible photolysis ($\lambda = 200-800$ nm).

be shown to arise from the four products $M{\cdot}NH_3$ (**1a**−**1c**), $HMNH_2$ (**2a**−**2c**), MNH_2 (**3a**−**3c**), and H_2MNH_2 (**4a**−**4c**), where M = Al, Ga, or In. Few of these monomeric molecules have been described previously in more than hypothetical terms, although amidogallane is familiar experimentally in its trimeric form, $[H_2GaNH_2]_3$, which is stable at temperatures up to nearly 150 °C.[3] The assignments will be justified by consideration of the frequencies and isotopic shifts of the observed bands and by comparisons either with the vibrational properties of the molecules anticipated by DFT calculations or with the vibrational properties reported for related species.

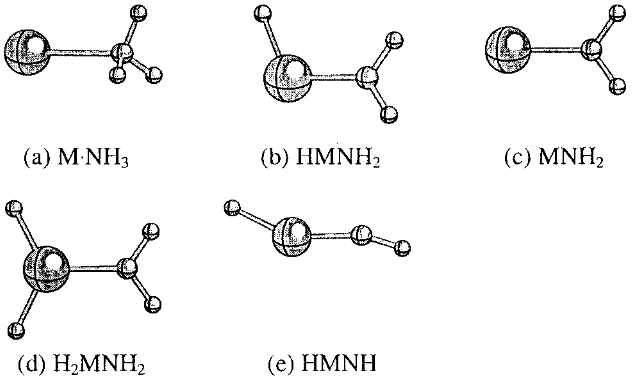
(a) $M{\cdot}NH_3$ (b) $HMNH_2$ (c) MNH_2

(d) H_2MNH_2 (e) HMNH

Figure 7. Calculated geometries of the molecules (a) $M{\cdot}NH_3$, (b) $HMNH_2$, (c) MNH_2, (d) H_2MNH_2, and (e) HMNH (M = Al, Ga, or In).

$M{\cdot}NH_3$ [M = Al (1a), Ga (1b), or In (1c)]. The observed IR signatures of each of the products **1a**, **1b,** and **1c**, formed on co-deposition of the metal atoms with ammonia, are wholly consistent with the presence of one or more NH_3 molecules perturbed by interaction with the metal. The conditions of the experiments were deliberately engineered to ensure that the matrices contained M atoms to the virtual exclusion of oligomers M_n.[14] Accordingly it seems unlikely that **1a**, **1b,** or **1c** contains more than one M atom. That the intensities of both the IR and visible absorptions should vary roughly in *direct* proportion to the matrix concentration of ammonia argues strongly, moreover, for the formulation of each of these species as $M{\cdot}NH_3$.

DFT calculations find a global minimum for the ground state of such a molecule with the geometry represented in Figure 7a; the optimized dimensions and vibrational properties are given in Table 4. As expected, each of the molecules resembles $Al{\cdot}NH_3$[23,24] in deviating slightly from regular C_{3v} symmetry;

Table 4. Comparison between the IR Spectra Observed and Calculated (Frequencies in cm^{-1}) for $M\cdot{}^{14}NH_3/M\cdot{}^{15}NH_3/M\cdot{}^{14}ND_3$ (**1a**−**1c**) (M = Al, Ga, or In)

$M\cdot{}^{14}NH_3$		$M\cdot{}^{15}NH_3$		$M\cdot{}^{14}ND_3$				
obsd	calcd[a]	obsd	calcd[a]	obsd	calcd[a]	assignment	description of vibrational mode	M
3447.1	3573.1 (43)	*b*	3563.1 (43)	*b*	2632.9 (22)	ν_1 (a′)	ν_{asym}(N−H)	Al
b	3458.2 (3)	*b*	3456.0 (2)	*b*	2470.1 (4)	ν_2 (a′)	ν_{sym}(N−H)	
b	1722.4 (31)	*b*	1719.2 (32)	*b*	1247.9 (13)	ν_3 (a′)	$\delta_{asym}(NH_3)$	
1131.4	1231.0 (174)	1125.6	1224.5 (170)	972.6	936.3 (122)	ν_4 (a′)	$\delta_{sym}(NH_3)$	
b	429.9 (8)	*b*	428.5 (8)	*b*	318.7 (4)	ν_5 (a′)	$\rho(NH_3)$	
b	244.8 (27)	*b*	240.7 (26)	*b*	232.8 (23)	ν_6 (a′)	ν(Al−N)	
b	3544.0 (5)	*b*	3535.2 (5)	*b*	2599.7 (2)	ν_7 (a″)	ν_{asym}(N−H)	
1593.6	1600.1 (20)	*b*	1597.5 (20)	*b*	1156.4 (8)	ν_8 (a″)	$\delta_{asym}(NH_3)$	
b	250.5 (1)	*b*	249.6 (1)	*b*	187.0 (0)	ν_9 (a″)	$\rho(NH_3)$	
3441.5	3594.3 (29)	*b*	3584.3 (29)	*b*	2648.0 (16)	ν_1 (a′)	ν_{asym}(N−H)	Ga
b	3473.6 (5)	*b*	3471.4 (5)	*b*	2480.7 (6)	ν_2 (a′)	ν_{sym}(N−H)	
b	1728.9 (30)	*b*	1725.7 (30)	*b*	1253.6 (14)	ν_3 (a′)	$\delta_{asym}(NH_3)$	
1104.2	1189.4 (153)	1099.1	1183.1 (150)	824.9	906.1 (107)	ν_4 (a′)	$\delta_{sym}(NH_3)$	
b	368.0 (15)	*b*	366.9 (15)	*b*	271.6 (6)	ν_5 (a′)	$\rho(NH_3)$	
b	204.7 (17)	*b*	200.1 (17)	*b*	191.4 (14)	ν_6 (a′)	ν(Ga−N)	
b	3565.5 (2)	*b*	3556.5 (2)	*b*	2617.0 (1)	ν_7 (a″)	ν_{asym}(N−H)	
1580.7	1590.6 (12)	1576.9	1587.8 (13)	*b*	1151.2 (5)	ν_8 (a″)	$\delta_{asym}(NH_3)$	
b	279.7 (9)	*b*	278.7 (9)	*b*	207.4 (3)	ν_9 (a″)	$\rho(NH_3)$	
3424.4	3542.3 (24)	3413.0	3532.7 (24)	*b*	2593.9 (14)	ν_1 (a′)	ν_{asym}(N−H)	In
b	3414.7 (4)	*b*	3412.4 (3)	*b*	2437.2 (5)	ν_2 (a′)	ν_{sym}(N−H)	
b	1683.8 (30)	*b*	1680.7 (30)	*b*	1217.1 (15)	ν_3 (a′)	$\delta_{asym}(NH_3)$	
1082.9	1171.7 (133)	1077.7	1165.4 (130)	816.0	884.5 (90)	ν_4 (a′)	$\delta_{sym}(NH_3)$	
b	291.2 (26)	*b*	290.2 (26)	*b*	214.0 (11)	ν_5 (a′)	$\rho(NH_3)$	
b	157.8 (16)	*b*	154.0 (15)	*b*	143.6 (13)	ν_6 (a′)	ν(In−N)	
b	3521.5 (6)	*b*	3512.7 (6)	*b*	2571.9 (3)	ν_7 (a″)	ν_{asym}(N−H)	
b	1451.0 (4)	*b*	1448.6 (4)	*b*	1046.4 (2)	ν_8 (a″)	$\delta_{asym}(NH_3)$	
b	252.4 (13)	*b*	251.6 (13)	*b*	185.5 (5)	ν_9 (a″)	$\rho(NH_3)$	

[a] $Al\cdot NH_3$ symmetry C_s: Al−N 2.3344 Å, N−H(1) 1.0162 Å, N−H(2,3) 1.0168 Å, Al−N−H(1) 114.2°, Al−N−H(2,3) 109.9°. $Ga\cdot NH_3$ symmetry C_s: Ga−N 2.4560 Å, N−H(1) 1.0148 Å, N−H(2,3) 1.0157 Å, Ga−N−H(1) 113.9°, Ga−N−H(2,3) 109.9°. $In\cdot NH_3$ symmetry C_s: In−N 2.7084 Å, N−H(1) 1.0244 Å, N−H(2,3) 1.0252 Å, In−N−H(1) 114.3°, In−N−H(2,3) 111.2°. Intensities (km mol^{-1}) are given in parentheses. [b] Too weak to be detected or hidden by ammonia absorptions or out of range of detection.

this is achieved through one N−H bond being slightly shorter than the other two and the H−N−H angles being fractionally different so that the overall symmetry is C_s and there are as a result not 6 but 9 distinct vibrational fundamentals. At 2.3344, 2.4560, and 2.7084 Å, the calculated M···N distances in $Al\cdot NH_3$, $Ga\cdot NH_3$, and $In\cdot NH_3$, respectively, come as something of a surprise, being about 1 Å shorter than the sum of the relevant van der Waals radii and implying a far from insignificant interaction between the two centers.

Comparisons between the IR spectra observed and those predicted are limited by the weakness of many of the transitions in IR absorption and by the masking effects of ammonia or water bands. Nevertheless, the features that could be detected for each complex were in satisfactory agreement with the properties forecast by the DFT calculations. Identifiable with the symmetric NH_3 deformation, ν_2 (a_1), is the band at 1131.4 cm^{-1} for **1a**, at 1104.2 cm^{-1}, for **1b** and at 1082.9 cm^{-1} for **1c**. These assignments are supported by the responses to isotopic change. With respect to ν_2 of matrix-isolated NH_3 at 974.5 cm^{-1}, therefore, we find *blue* shifts of 156.9, 129.7 and 108.4 cm^{-1} for **1a**, **1b,** and **1c**, respectively. Similar in sense but smaller in magnitude, these features show parallels with the vibrational properties of NH_3 molecules coordinated to metal cations[38] and therefore imply M···N interaction between the metal and ammonia molecules in **1a**, **1b,** and **1c**. Hence the ammonia adducts of Al, Ga, and In exhibit a $\delta_{sym}(NH_3)$ mode with a blue shift similar to those observed previously[47] for the alkali metal adducts $Li\cdot NH_3$, $Na\cdot NH_3$, $K\cdot NH_3$, and $Cs\cdot NH_3$. The bands at 3447.1 cm^{-1} for **1a**, at 3441.5 cm^{-1} for **1b**, and at 3424.4 cm^{-1} for **1c** are identifiable with the antisymmetric N−H stretching fundamental, ν_1 (a′). The ^{15}N shift of -11.4 cm^{-1} observed for **1c** confirms this assignment. Thus, the frequencies are close to that of the corresponding ν_3 (e) fundamental of uncoordinated NH_3 (3434.0 cm^{-1}).[33] This observation is in general agreement with the results of our DFT calculations [3585.3 cm^{-1} for ν_3 (e) in NH_3; 3573.1, 3594.3, and 3542.3 cm^{-1} for ν_1 (a′) in $Al\cdot NH_3$, $Ga\cdot NH_3$, and $In\cdot NH_3$, respectively]. In the case of the alkali metals, the symmetric N−H stretching mode was observed to be the most intense feature in the spectra of the adducts. For the group 13 metal adducts, however, the calculations indicate that ν_{asym}(N−H) gives the most intense IR absorption in this region. We have also calculated the IR spectrum of $Li\cdot NH_3$ (C_{3v} symmetry; Li−N 1.9933, N−H 1.0210 Å; H−N−H 106.7°), with the following results (frequencies in cm^{-1}, intensities in km mol^{-1} in brackets): ν_{asym}(N−H) NH_3 3585.3 (3), $Li\cdot NH_3$ 3496.6 (64); ν_{sym}(N−H) NH_3 3464.2 (1), $Li\cdot NH_3$ 3381.1 (586); $\delta_{sym}(NH_3)$ NH_3 1122.7 (202), $Li\cdot NH_3$ 1252.0 (105.7). The large increase in intensity of the absorptions of ammonia brought about by coordination has been previously correlated with the degree of metal-to-ligand charge transfer in the adduct.[46] On the basis of this correlation, the degree of charge transfer appears, as expected, to be considerably higher in the alkali metal adducts than in the group 13 metal adducts.

The third absorption present in the spectra of **1a** and **1b** (at 1593.6 and 1580.7 cm^{-1}) is identifiable with the $\delta_{asym}(NH_3)$ mode of $Al\cdot NH_3$ and $Ga\cdot NH_3$, respectively. It was not possible unfortunately to locate a transition corresponding to the ν(M−N) fundamental, which is not expected to be very intense in IR absorption and, with a predicted frequency of 244.8, 204.7, or 157.8 cm^{-1} for Al, Ga, or In, respectively, is likely to fall below the low-frequency threshold of detection (200 cm^{-1}) in our experiments.

---

(46) Süzer, S.; Andrews, L. *J. Am. Chem. Soc.* **1987**, *109,* 300−304.

We have investigated possible excited states of Ga•NH_3 in order to determine the likely origin and photochemical role of the electronic transition near 440 nm. On the evidence available, we believe this and the related features of Al•NH_3 and In•NH_3 to be essentially a metal-based $^2S \leftarrow {}^2P$ transition appreciably red-shifted by the coordinating action of the NH_3 molecule. The reaction energies for the formation of the adducts starting from the metal atom in its ^2P ground state and NH_3 were found to be −60.2, −51.8, and −28.8 kJ mol^{-1} for M = Al, Ga, and In, respectively.

$HMNH_2$ [M = Al (2a), Ga (2b), or In (2c)]. As noted previously, the IR bands at 1761.1, 1721.8, and 1533.8 cm^{-1} are highly suggestive of a ν(M−H) fundamental of **2a** (M = Al), **2b** (M = Ga), and **2b** (M = In), respectively, where M is in a *divalent* state. The observed H/D ratios of 1.3731 for **2a**, 1.3780:1 for **2b**, and 1.3833:1 for **2c** are in keeping with those for other monohydrides, e.g., CH_3GaH 1.3827:1,[14] CH_3InH 1.3864:1,[14] $HFeNH_2$ 1.3890:1,[21] and $HNiNH_2$ 1.3401:1.[22] The aluminum compound $HAlNH_2$ has been reported previously, having been identified by its IR spectrum in argon matrices containing laser-ablated Al atoms and NH_3;[19] the results presented here generally tally with, but are more extensive than, those of the earlier study.

The absorption at 1533.6 cm^{-1} (H/D ratio 1.3319:1) is characteristic of an NH_2 scissoring mode of **2a**,[38] thus pointing to the presence of an NH_2 fragment. What appears to be the ν_{sym}(N−H) mode of the NH_2 group, located at 3476.4 cm^{-1} (H/D ratio 1.3393:1), was also detected. Support for these assignments comes from the $^{14}N/^{15}N$ shifts of the two bands (−2.1 and −8.2 cm^{-1}, respectively). Next in order of decreasing frequency comes the signal at 778.7 cm^{-1}, which can be assigned to the ν(Al−N) fundamental on the basis of its H/D ratio (1.0406:1) and its ^{15}N shift (−11.8 cm^{-1}). The observation of these bands gives strong grounds for believing that **2a** is $HAlNH_2$. The signal at 705.2 cm^{-1} (H/D ratio 1.2826, ^{15}N shift −4.2 cm^{-1}) is then attributable to an NH_2 wagging fundamental. The features at 483.8 and 393.8 cm^{-1}, with H/D ratios of 1.3962:1 and 1.2928:1 and $^{14}N/^{15}N$ shifts of −0.6 and −1.9 cm^{-1}, respectively, can be assigned to the NH_2 out-of-plane rock and the Al−H out-of-plane deformation modes. Unfortunately, however, the D- and ^{15}N-counterparts to the obvious candidate for the Al−H in-plane deformation mode at 482.2 cm^{-1} were too weak to be observed.

Besides the band at 1721.8 cm^{-1} suggesting the presence of a Ga(II)−H bond, the spectrum of **2b** also includes numerous signs of the NH_2 ligand. For example, the feature at 3485.4 cm^{-1} in the spectrum of the ^{15}N isotopomer is most obviously ascribed to a ν(N−H) mode, that at 1528.7 cm^{-1} in the spectrum of the normal isotopomer to the scissoring mode of the NH_2 fragment. Strong support for the second of these assignments comes not only from the H/D ratio (1.3351:1) and ^{15}N shift of −2.5 cm^{-1}, but also from the frequencies (in cm^{-1}) reported for the corresponding mode of the following species: $HAlNH_2$ 1533.6 (H/D = 1.3319:1), $HFeNH_2$ 1517.8 (H/D = 1.3412:1),[21] and $HNiNH_2$ 1533.3 (H/D = 1.3021:1).[22] Analogy with $HAlNH_2$ suggests that the band at 746.2 cm^{-1} represents the NH_2 wagging mode of **2b**, although the H/D ratio of 1.3242:1 is rather larger than that (1.2826:1) for the aluminum compound. Evidence of $^{69}Ga/^{71}Ga$ splitting and a large ^{15}N shift (−15.7 cm^{-1}) make the feature at 668.5/667.4 cm^{-1} the obvious candidate for a ν(Ga−N) mode. Given the conditions leading to the formation of the compound and analogies with the photochemical changes shown to occur in the systems Al/NH_3 and M/CH_4 (M = Al, Ga, or In),[14] the most plausible interpretation of these properties is that **2b** is $HGaNH_2$ formed in accordance with the insertion reaction 2. The reaction energies for the formation of $HMNH_2$ by tautomerization of the ammonia adducts were calculated to be −79.6, +13.1, and +37.8 kJ mol^{-1} for M = Al, Ga, and In, respectively.

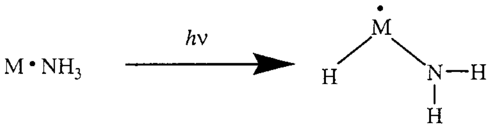

(2)

The indium compound **2c** shows features similar to those observed for **2a** and **2b**. The absorption at 1512.9 cm^{-1} (H/D = 1.3482:1) corresponds to the NH_2 scissoring mode, whereas that at 709.0 cm^{-1} (H/D = 1.3559:1) is the obvious choice for the NH_2 wagging mode. There is also a signal at 564.8 cm^{-1} which, with a ^{15}N shift of −13.1 cm^{-1} and an H/D ratio of 1.0681:1, has the right credentials to correspond to what is mainly a ν(In−N) vibration.

DFT calculations find an equilibrium geometry with C_s symmetry for each of the molecules $HAlNH_2$ and $HGaNH_2$, as illustrated in Figure 7b. The equilibrium geometry of $HInNH_2$ exhibits only C_1 symmetry with the M−NH_2 fragment having the form of a shallow pyramid. The dimensions of all three species are given in Table 5. The H−M−N skeleton is bent with an H−M−N angle of 115.5, 116.3, or 115.5° for M = Al, Ga, or In; the M−N bonds are relatively short (measuring 1.7880, 1.8362, and 1.9929 Å for M = Al, Ga, and In, respectively).

Out of the nine IR-active vibrational fundamentals expected for each of the $HMNH_2$ molecules, no less than eight, seven, and five have been observed for $HAlNH_2$, $HGaNH_2$, and $HInNH_2$, respectively, as one or other of their different isotopomers. The relative intensities, frequencies, and isotopic shifts are found to be in generally excellent agreement with the properties predicted for the optimized ground state of the molecules by DFT/B3LYP calculations. Hence, as indicated in Table 5, we have succeeded in locating and assigning all the fundamental bands in the range 420−4000 cm^{-1} calculated to have intensities in excess of 10 km mol^{-1}. On this basis we can confirm that the modes approximating most closely to ν(Ga−N) and ν(In−N) vibrations occur at 668.5/667.4 and 564.8 cm^{-1}, respectively, predictably lying at lower frequency than the ν(Al−N) fundamental of $HAlNH_2$ (778.7 cm^{-1}).

MNH_2 [M = Al (3a), Ga (3b), or In (3c)]. Irradiation with broad-band UV−visible light (λ = 200−800 nm) results in the efficient conversion of $HMNH_2$ to a new product, viz., **3a** (M = Al), **3b** (M = Ga), or **3c** (M = In), which lacks any spectroscopic sign of an M−H bond. That it nevertheless retains a coordinated NH_2 group is implied by the observation of IR bands with frequencies and isotopic shifts appropriate to their attribution either to internal vibrations of the NH_2 ligand (3495.1 and 1520.3 cm^{-1} for **3a**, 3471.6 and 1505.9 cm^{-1} for **3b**, and 3481.7 and 1498.1 cm^{-1} for **3c**) or to an M−N stretching vibration (726.5, 589.3/587.9, and 498.7 cm^{-1} for **3a**, **3b,** and **3c**, respectively). The obvious inference is that **3a** is the simple aluminum(I) amide, $AlNH_2$, and **3b** and **3c** are the corresponding gallium and indium compounds, $GaNH_2$ and $InNH_2$, each formed by photodissociation of the M−H bond in $HMNH_2$ in accordance with reaction 3, plainly analogous to eq 1. $AlNH_2$ has been identified in an earlier matrix study[19] with results that match closely, but are somewhat less extensive than, the ones reported here. As with the formation of CH_3M from CH_3MH

Table 5. Comparison between the IR Spectra Observed and Calculated (Frequencies in cm^{-1}) for $HM^{14}NH_2$/$HM^{15}NH_2$/$DM^{14}ND_2$ (**2a**−**2c**) (M = Al, Ga, or In)

$HM^{14}NH_2$		$HM^{15}NH_2$		$DM^{14}ND_2$				
obsd	calcd[a]	obsd	calcd[a]	obsd	calcd[a]	assignment	description of vibrational mode	M
3476.4	3645.1 (14)	3468.2	3634.9 (14)	2595.6	2685.8 (11)	ν_1 (a′)	ν_{sym}(N−H)	Al
b	3551.1 (4)	*b*	3545.9 (4)	*b*	2568.9 (8)	ν_2 (a′)	ν_{asym}(N−H)	
1761.1	1820.5 (205)	1761.0	1820.5 (205)	1282.6	1312.0 (117)	ν_3 (a′)	ν(Al−H)	
1533.6	1620.4 (41)	1531.5	1615.1 (39)	1151.4	1208.4 (40)	ν_4 (a′)	NH_2 scissoring	
778.7	795.0 (86)	766.9	781.5 (93)	748.3	752.1 (52)	ν_5 (a′)	ν(Al−N)	
705.2	746.9 (116)	701.0	742.2 (107)	549.8	580.3 (72)	ν_6 (a′)	NH_2 wagging	
482.2	486.5 (27)	*b*	486.3 (27)	*b*	348.4 (14)	ν_7 (a′)	Al−H in-plane def.	
483.8	498.3 (31)	483.2	497.4 (28)	346.5	366.3 (56)	ν_8 (a″)	NH_2 out-of-plane rock	
393.8	426.5 (226)	391.9	424.4 (227)	304.6	323.3 (94)	ν_9 (a″)	Al−H out-of-plane def.	
b	3664.2 (14)	3485.4	3653.7 (14)	*b*	2703.3 (11)	ν_1 (a′)	ν_{sym}(N−H)	Ga
b	3551.5 (4)	*b*	3546.6 (4)	*b*	2566.3 (7)	ν_2 (a′)	ν_{asym}(N−H)	
1721.8	1759.3 (189)	1721.8	1759.2 (189)	1249.5	1254.3 (103)	ν_3 (a′)	ν(Ga−H)	
1528.7	1601.3 (21)	1523.2	1596.2 (20)	1145.0	1191.1 (23)	ν_4 (a′)	NH_2 scissoring	
746.2	752.2 (78)	743.7	748.1 (79)	563.5	573.8 (50)	ν_5 (a′)	NH_2 wagging	
668.5	665.0 (59)	652.8	649.3 (56)	626.6	626.8 (41)	ν_6 (a′)	ν(^{69}Ga−N)	
b	479.8 (6)	*b*	479.6 (6)	*b*	342.3 (5)	ν_7 (a′)	Ga−H in-plane def.	
494.1	481.0 (21)	494.1	481.0 (26)	*b*	342.9 (12)	ν_8 (a″)	NH_2 out-of-plane rock	
210.9	229.1 (238)	*b*	227.6 (235)	*b*	176.6 (136)	ν_9 (a″)	Ga−H out-of-plane def.	
3463.5	3597.6 (15)	*b*	3587.4 (15)	*b*	2651.8 (13)	ν_1 (a)	ν_{sym}(N−H)	In
b	3486.0 (5)	*b*	3481.0 (4)	*b*	2519.4 (8)	ν_2 (a)	ν_{asym}(N−H)	
1533.8	1580.6 (197)	1533.8	1580.0 (203)	1108.8	1121.1 (98)	ν_3 (a)	ν(In−H)	
1512.9	1567.7 (28)	*b*	1563.5 (21)	1122.2	1162.9 (31)	ν_4 (a)	NH_2 scissoring	
709.0	682.5 (97)	*b*	679.2 (96)	522.9	513.1 (73)	ν_5 (a)	NH_2 wagging	
564.8	555.9 (57)	551.7	541.9 (54)	528.8	524.9 (33)	ν_6 (a)	ν(In−N)	
b	407.5 (13)	*b*	407.4 (13)	*b*	290.3 (8)	ν_7 (a)	NH_2 out-of-plane rock	
b	425.0 (40)	*b*	424.9 (40)	*b*	302.8 (18)	ν_8 (a)	In−H in-plane def.	
b	154.2 (190)	*b*	153.1 (187)	*b*	119.7 (112)	ν_9 (a)	In−H out-of-plane def.	

[a] $HAlNH_2$ symmetry C_s: Al−H 1.6050 Å, Al−N 1.7880 Å, N−H 1.0112/1.0098 Å, H−Al−N 115.5°, Al−N−H 124.6/125.3°. $HGaNH_2$ symmetry C_s: Ga−H 1.6019 Å, Ga−N 1.8362 Å, N−H 1.0112/1.0087 Å, H−Ga−N 116.3°, Ga−N−H 124.0/124.3°. Frequencies (in cm^{-1}) calculated for $H^{71}Ga^{14}NH_2$: 3664.2 (14), 3551.5 (4), 1758.9 (189), 1601.3 (21), 752.0 (78), 663.3 (59), 479.8 (6), 480.9 (26), 229.0 (238). $HInNH_2$ symmetry C_1: In−N 1.9929 Å, In−H 1.7676 Å, N−H 1.0178/1.0203 Å, H−In−N 115.5°, In−N−H 123.8/123.1°, H−In−N−H 15.7/172.2°. Intensities (km mol^{-1}) are given in parentheses. [b] Too weak to be detected or hidden by ammonia absorptions or out of range of detection.

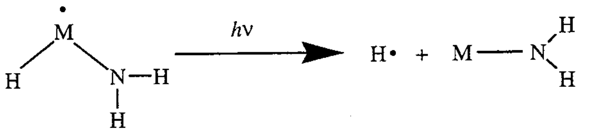

(3)

under similar circumstances,[14] the hydrogen atom expelled in this process is presumably enabled by its small size to escape from the matrix cage; it is also a potential source of secondary change.

DFT calculations have identified a global minimum corresponding to an equilibrium geometry for each of the MNH_2 molecules with a planar skeleton and C_{2v} symmetry (see Figure 7c). The planar geometry at nitrogen, together with the relatively short M−N bonds in group 13 species of this type [r(M−N) = 1.8131, 1.8836, and 2.0389 Å for M = Al, Ga, and In, respectively], appears again to signify that N to M π-interactions contribute to the M−N bonding. There are therefore six distinct IR-active vibrational fundamentals spanning the representation $3a_1 + 1b_1 + 2b_2$. Our experiments have identified IR absorptions with frequencies, relative intensities, and isotopic shifts in good agreement with those predicted for no less than four of the fundamentals of each of the molecules $AlNH_2$, $GaNH_2$, and $InNH_2$. Guided by the calculations, the isotopic shifts, and analogies with the spectra of related compounds, we arrive with some assurance at the assignments of the observed features set out in Table 6. Hence the NH_2 scissoring fundamental, ν_2 (a_1), and the M−N stretching mode, ν_3 (a_1), are found to take the following frequencies (in cm^{-1}): $AlNH_2$, $\nu_2 = 1520.3$, $\nu_3 = 726.5$; $GaNH_2$, $\nu_2 = 1505.9$, $\nu_3 = 589.3/587.9$; $InNH_2$, $\nu_2 = 1498.1$, $\nu_3 = 498.7$. When the frequencies are translated into force constants, we find that while f_{MN} maintains the order Al > Ga > In, the values are significantly smaller for the univalent species MNH_2 than for the corresponding divalent one $HMNH_2$. This difference is also reflected in the slightly longer M−N bond distance in MNH_2. A similar pattern is displayed by the M−C bonds in the molecules CH_3MH and CH_3M, where M = Al, Ga, or In.[14]

H_2MNH_2 [M = Al (4a), Ga (4b), or In (4c)]. Of the possible isomers with the composition MNH_4, that with the planar, ethene-like structure H_2MNH_2 (Figure 7d) is lowest in energy by some margin, according to DFT calculations employing the B3LYP hybrid method. Details of the calculated dimensions and the corresponding vibrational frequencies are given in Table 7. The structure in each case is thus analogous to that deduced previously by both theory[9] and experiment[8] for the corresponding boron compound H_2BNH_2; there is also good agreement with the results of earlier calculations (using, for example, SCF methods and CISD and CCSD levels of theory) taking in the aluminum compound.[24,26,28] The planar H_2MNH_2 unit conforms to C_{2v} symmetry with the result that its 12 vibrational fundamentals are accommodated by the representation $5a_1 + 1a_2 + 2b_1 + 4b_2$. Of the 11 IR-active modes ($5a_1 + 2b_1 + 4b_2$), all but two have been satisfactorily identified in the spectra measured for H_2AlNH_2 (**4a**) and all but one have been so identified in the spectra measured for H_2GaNH_2 (**4b**). In these two cases the transitions that have escaped detection have probably been obscured by more intense absorptions due to the other molecules present in the matrices. Only with H_2InNH_2, invariably formed in low concentrations, are the observed transitions exceeded in number by the unobserved ones, mainly for want of intensity but partly also for reasons of frequency

Table 6. Comparison between the IR Spectra Observed and Calculated (Frequencies in cm^{-1}) for $M^{14}NH_2$/$M^{15}NH_2$/$M^{14}ND_2$ (**3a**−**3c**) (M = Al, Ga, or In)

$M^{14}NH_2$		$M^{15}NH_2$		$M^{14}ND_2$				
obsd	calcd[a]	obsd	calcd[a]	obsd	calcd[a]	assignment	description of vibrational mode	M
b	3503.7 (0.06)	*b*	3498.6 (0.15)	*b*	2534.6 (2)	ν_1 (a_1)	ν_{sym}(N-H)	Al
1520.3	1614.0 (63)	1515.0	1608.7 (60)	1137.8	1202.6 (64)	ν_2 (a_1)	NH_2 scissoring	
726.5	735.1 (81)	713.6	721.9 (79)	694.9	698.2 (64)	ν_3 (a_1)	ν(Al−N)	
406.5	469.3 (263)	403.9	466.2 (260)	314.6	364.7 (149)	ν_4 (b_1)	out-of-plane def.	
3495.1	3590.3 (6)	3486.2	3580.4 (6)	*b*	2643.5 (3)	ν_5 (b_2)	ν_{asym}(N-H)	
b	499.0 (0.1)	*b*	496.8 (0.1)	*b*	377.4 (0.01)	ν_6 (b_2)	$\rho(NH_2)$	
b	3499.8 (1)	*b*	3494.2 (0.7)	*b*	2528.7 (1)	ν_1 (a_1)	ν_{sym}(N−H)	Ga
1505.9	1599.9 (32)	1501.2	1595.0 (30)	1132.6	1189.5 (40)	ν_2 (a_1)	NH_2 scissoring	
589.3	595.2 (94)	574.3	581.0 (89)	557.9	560.8 (78)	ν_3 (a_1)	$\nu(^{69}Ga{-}N)$	
303.3	363.5 (283)	302.7	362.7 (280)	*b*	282.5 (164)	ν_4 (b_1)	out-of-plane def.	
3471.6	3599.7 (2)	*b*	3588.7 (3)	*b*	2652.1 (1)	ν_5 (b_2)	ν_{asym}(N−H)	
b	509.0 (1)	*b*	507.3 (1)	*b*	382.4 (0.4)	ν_6 (b_2)	$\rho(NH_2)$	
b	3446.0 (0.5)	*b*	3441.2 (1)	*b*	2490.6 (1)	ν_1 (a_1)	ν_{sym}(N−H)	In
1498.1	1568.1 (26)	1493.6	1563.3 (24)	1116.3	1160.8 (33)	ν_2 (a_1)	NH_2 scissoring	
498.7	504.3 (93)	488.2	491.3 (89)	480.6	475.3 (80)	ν_3 (a_1)	ν(In−N)	
237.0	256.3 (236)	235.4	254.6 (233)	*b*	198.3 (139)	ν_4 (b_1)	out-of-plane def.	
3481.7	3548.3 (4)	*b*	3538.4 (4)	*b*	2613.3 (3)	ν_5 (b_2)	ν_{asym}(N−H)	
469.6	447.8 (3)	*b*	445.9 (3)	*b*	335.1 (1)	ν_6 (b_2)	$\rho(NH_2)$	

[a] $AlNH_2$ symmetry C_{2v}: Al−N 1.8131 Å, N−H 1.0149 Å, H−N−H 108.5°. $GaNH_2$ symmetry C_{2v}: Ga−N 1.8836 Å, N−H 1.0145 Å, H−N−H 109.3°. Frequencies (in cm^{-1}) calculated for $^{71}GaNH_2$: 3598.9 (3), 3499.1 (0.5), 1600.2 (32), 593.5 (93), 509.4 (1), 365.9 (283). $InNH_2$ symmetry C_{2v}: In−N 2.0389 Å, N−H 1.0227 Å, H−N−H 107.9°. Intensities (km mol^{-1}) are given in parentheses. [b] Too weak to be detected or hidden by ammonia absorptions.

(i.e., outside the experimental limits of 4000−200 cm^{-1}) or of masking by the absorptions of other species.

The calculated frequencies and relative intensities have then played a central role in guiding the assignment of the IR absorptions displayed by the molecules **4a**−**4c**. Validation of the proposed assignments comes mainly from the measured isotopic shifts, with supporting evidence being provided by analogies with the vibrational properties already established for related molecules [e.g., MH_3 (M = Al, Ga, or In),[10] H_2MCl (M = Ga[42] or In[15]), $HMNH_2$, and MNH_2 (M = Al, Ga, or In)]. The ability of the calculations to reproduce the frequencies (with rms deviations of no more than 3.3 and 5.8% for **4a** and **4b**, respectively), isotopic shifts, and intensity patterns of the observed spectra would appear to confirm the identities and geometries of the aluminum and gallium compounds, with strong circumstantial grounds for presuming that in the compound **4c** indium follows suit. Best defined by its measured vibrational properties is the gallium compound, **4b**, and just how well experiment generally matches theory may be gauged by the ^{15}N shifts (all negative and in cm^{-1}) displayed by the following bands (with frequencies also in cm^{-1}) presented in parentheses in the order exptl/calcd: 3510.7 (10.0/10.8), 3413.4 (7.5/4.9), 1970.8 (0.1/0.1), 1530.4 (6.1/5.4), 782.8 (4.5/4.7), 779.6 (4.4/3.5), 706.2/704.1 (14.0/13.1), 567.7 (0.3/0.0), and 304.9 (2.1/2.4). In addition, the observed $^{69}Ga/^{71}Ga$ splitting of 2.1 cm^{-1} characterizing the absorption near 705 cm^{-1} matches admirably the calculated value of 1.9 cm^{-1} for what is essentially the ν(Ga−N) mode, ν_5 (a_1).

Two of the most prominent bands due to H_2AlNH_2—at 1899.3 and 1891.0 cm^{-1} —tally with features reported by Lanzisera and Andrews[19] in the course of their matrix studies of the reactions between laser-ablated Al atoms and NH_3. On that occasion they were assigned somewhat tentatively not to H_2AlNH_2 but to the nonlinear, high-energy isomer of $AlNH_2$, namely, HAlNH. Laser ablation produces highly energetic Al atoms, including some that are electronically excited, and the odds are that the compound **4a** would be formed, at least as a minor product, in the earlier experiments. With no less than nine IR bands now traceable to this species, including several features characteristic of an NH_2 group, it would be hard to reconcile our observations with HAlNH, a molecule having the potential for no more than six distinct IR-active fundamentals. Nevertheless, we have extended our DFT calculations to include molecules of the type HMNH (M = Al, Ga, or In), thereby securing the optimum geometry illustrated in Figure 7e. Hence we confirm that such molecules are indeed high-energy species, being less stable than MNH_2 by 177.7, 188.4, and 257.5 kJ mol^{-1} for M = Al, Ga, and In, respectively. The geometries are invariably bent, with H−M−N angles near 160° and M−N−H angles near 120°, although the potential well is extremely shallow with respect to the bending coordinates. Despite the absence of the conventional signs of multiple π-bonding, the M−N bond is calculated (at 1.6271, 1.6989, and 1.8345 Å for M = Al, Ga, and In, respectively) to be shorter than in any other compound with the general formula MNH_n ($n = 2{-}6$). The most distinctive feature of the vibrational properties is the high frequency of the ν(M−H) fundamental, which is predicted, for example, to be about 100 cm^{-1} higher for HAlNH than for the corresponding modes of H_2AlNH_2. Hence a frequency near 2000 cm^{-1}, rather than 1900 cm^{-1}, as observed for **4a**, is to be expected for HAlNH. On the evidence of published work, therefore, we are doubtful whether this molecule, or any homologue of the heavier group 13 metals, has yet been sighted in the laboratory.

The signal at 1887.6 cm^{-1} in the experiments with Al and those at 1942.0 and 754.3 cm^{-1} in the experiments with Ga can be assigned either to an ammonia adduct of H_2MNH_2 or to the dimer $[H_2MNH_2]_2$. To gain more information about the possible dimerization $2H_2MNH_2 \rightarrow [H_2MNH_2]_2$ for M = Al or Ga, we have calculated the reaction energy, as well as the structure and IR spectra of the dimer. In each case, the dimer has a structure with D_{2h} symmetry and two bridging NH_2 units (bond length in Å, angles in deg: $[H_2AlNH_2]_2$ Al−H 1.5896, Al−N 1.9808, N−H 1.0162, Al···Al 2.8712, H−Al−H 123.3, N−Al−N 87.1, H−N−H 106.4; $[H_2GaNH_2]_2$ Ga−H 1.5710, Ga−N 2.0373, N−H 1.0152, Ga···Ga 2.9885, H−Ga−H 125.2, N−Ga−N 85.6, H−N−H 106.7). Both processes are exothermic with reaction energies of 197.1 kJ mol^{-1} for Al and 240.6 kJ mol^{-1} for Ga, much higher than the estimated energy for the formation of Ga_2H_6 from two GaH_3 molecules (92.8 kJ

Table 7. Comparison between the IR Spectra Observed and Calculated (Frequencies in cm^{-1}) for $H_2M^{14}NH_2/H_2M^{15}NH_2/D_2M^{14}ND_2$ (**4a**−**4c**) (M = Al, Ga, or In)

$H_2M^{14}NH_2$		$H_2M^{15}NH_2$		$D_2M^{14}ND_2$				
obsd	calcd[a]	obsd	calcd[a]	obsd	calcd[a]	assignment	description of vibrational mode	M
3499.7	3572.0 (11)	*b*	3566.9 (10)	*b*	2583.9 (13)	ν_1 (a_1)	ν_{sym}(N−H)	
1891.0	1959.3 (81)	1891.1	1959.3 (81)	*b*	1398.2 (58)	ν_2 (a_1)	ν_{sym}(Al−H)	
1541.6	1631.2 (49)	1536.1	1625.8 (47)	1159.5	1218.0 (46)	ν_3 (a_1)	$\delta(NH_2)$	
818.7	830.1 (192)	809.8	820.2 (214)	*b*	774.1 (72)	ν_4 (a_1)	ν(Al−N)	
755.0	754.6 (86)	*b*	749.6 (63)	548.4	548.7 (86)	ν_5 (a_1)	$\delta(AlH_2)$	
	499.9 (0)		499.9 (0)		353.6 (0)	ν_6 (a_2)	twist	Al
608.7	608.4 (150)	608.1	608.4 (149)	450.4	455.5 (124)	ν_7 (b_1)	$\rho_{out-of-plane}(AlH_2)$	
518.3	483.0 (309)	516.7	479.6 (306)	397.7	376.9 (149)	ν_8 (b_1)	$\rho_{out-of-plane}(NH_2)$	
b	3655.8 (11)	*b*	3645.5 (11)	*b*	2694.5 (11)	ν_9 (b_2)	ν_{asym}(N−H)	
1899.3	1964.2 (288)	1899.3	1964.2 (288)	1384.2	1426.6 (169)	ν_{10} (b_2)	ν_{asym}(Al−H)	
769.8	767.6 (151)	766.2	762.9 (150)	611.0	603.4 (88)	ν_{11} (b_2)	$\delta_{in-plane}(NH_2)$	
b	433.5 (22)	*b*	433.5 (22)	*b*	311.7 (10)	ν_{12} (b_2)	$\delta_{in-plane}(AlH_2)$	
3413.4	3581.9 (9)	3405.9	3577.0 (9)	*b*	2588.3 (11)	ν_1 (a_1)	ν_{sym}(N−H)	
1970.8	1995.9 (64)	*b*	1995.9 (64)	1407.7	1415.6 (33)	ν_2 (a_1)	ν_{sym}(Ga−H)	
1530.4	1621.6 (30)	1524.3	1616.2 (28)	1150.9	1208.6 (30)	ν_3 (a_1)	$\delta(NH_2)$	
779.6	740.3 (40)	775.2	736.8 (59)	568.8	519.8 (68)	ν_4 (a_1)	$\delta(GaH_2)$	
706.2	689.0 (124)	692.2	675.9 (103)	667.8	658.0 (21)	ν_5 (a_1)	$\nu(^{69}Ga-N)$	Ga
	545.8 (0)		545.8 (0)		386.1 (0)	ν_6 (a_2)	twist	
567.7	607.9 (43)	567.4	607.9 (43)	405.9	439.7 (26)	ν_7 (b_1)	$\rho_{out-of-plane}(GaH_2)$	
304.9	337.3 (280)	302.8	334.9 (277)	*b*	263.3 (161)	ν_8 (b_1)	$\rho_{out-of-plane}(NH_2)$	
3510.7	3681.7 (13)	3500.7	3670.9 (12)	*b*	2717.3 (12)	ν_9 (b_2)	ν_{asym}(N−H)	
1970.8	1998.6 (245)	1970.7	1998.5 (245)	1419.1	1428.3 (133)	ν_{10} (b_2)	ν_{asym}(Ga−H)	
782.8	789.8 (110)	778.3	785.1 (109)	605.1	608.8 (64)	ν_{11} (b_2)	$\delta_{in-plane}(NH_2)$	
b	441.8 (26)	*b*	441.7 (27)	*b*	316.2 (12)	ν_{12} (b_2)	$\delta_{in-plane}(GaH_2)$	
b	3517.1 (10)	*b*	3512.3 (9)	*b*	2541.6 (12)	ν_1 (a_1)	ν_{sym}(N−H)	
b	1770.2 (68)	*b*	1770.2 (68)	*b*	1254.1 (38)	ν_2 (a_1)	ν_{sym}(In−H)	
1506.6	1579.4 (23)	*b*	1574.5 (22)	*b*	1171.3 (24)	ν_3 (a_1)	$\delta(NH_2)$	
b	634.2 (84)	*b*	631.4 (106)	474.6	441.7 (110)	ν_4 (a_1)	$\delta(InH_2)$	
616.3	575.8 (153)	599.2	563.4 (128)	*b*	553.4 (28)	ν_5 (a_1)	ν(In−N)	
	480.8 (0)		480.8 (0)		340.1 (0)	ν_6 (a_2)	twist	In
b	535.2 (95)	*b*	535.2 (94)	*b*	384.0 (52)	ν_7 (b_1)	$\rho_{out-of-plane}(InH_2)$	
c	177.6 (237)	*c*	176.3 (234)	*c*	139.5 (140)	ν_8 (b_1)	$\rho_{out-of-plane}(NH_2)$	
b	3621.9 (18)	*b*	3611.5 (17)	*b*	2671.3 (17)	ν_9 (b_2)	ν_{asym}(N−H)	
1805.9	1756.9 (272)	1805.9	1756.9 (272)	1299.0	1250.7 (141)	ν_{10} (b_2)	ν_{asym}(In−H)	
733.3	696.3 (126)	731.4	692.2 (125)	*b*	534.1 (76)	ν_{11} (b_2)	$\delta_{in-plane}(NH_2)$	
b	368.5 (33)	*b*	368.4 (34)	*b*	263.3 (16)	ν_{12} (b_2)	$\delta_{in-plane}(InH_2)$	

[a] H_2AlNH_2 symmetry C_{2v}: Al−N 1.7790 Å, Al−H 1.5811 Å, N−H 1.0100 Å, H−Al−H 124.4°, H−N−H 110.0°. H_2GaNH_2 symmetry C_{2v}: Ga−N 1.8211 Å, Ga−H 1.5621 Å, N−H 1.0086 Å, H−Ga−H 126.7°, H−N−H 111.7°. Frequencies (in cm^{-1}) calculated for $H_2{}^{71}GaNH_2$: 3681.7 (13), 3581.9 (9), 1998.0 (242), 1995.8 (67), 1621.6 (30), 789.5 (110), 740.2 (41), 687.1 (122), 607.5 (42), 545.8 (0), 441.7 (26), 337.2 (278). H_2InNH_2 symmetry C_{2v}: In−N 1.9703 Å, In−H 1.7252 Å, N−H 1.0169 Å, H−In−H 126.9°, H−N−H 110.3°. Intensities (km mol^{-1}) are given in parentheses. [b] Too weak to be detected or hidden by ammonia absorptions. [c] Out of range of detection.

mol^{-1}). However, as for the dimerization of GaH_3, a substantial reaction barrier is likely to prohibit the reaction in a solid argon matrix. The calculations gave the following frequencies for the most intense IR absorptions [values in cm^{-1} with intensities (km mol^{-1}) in brackets]: $[H_2AlNH_2]_2$ 1922.3 (634) b_{1u}, 1915.0 (230) b_{3u}, 901.1 (613) b_{3u}, 763.1 (214) b_{1u}, 762.3 (651) b_{2u}, 738.0 (421) b_{3u}; $[H_2GaNH_2]_2$ 1958.2 (548) b_{1u}, 1949.7 (274) b_{3u}, 894.7 (334) b_{3u}, 720.1 (250) b_{3u}, 717.1 (165) b_{1u}, 702.5 (347) b_{2u}. Annealing the matrices did not lead to a significant change in the intensities of any signals. The observation of the absorptions at 1887.6, 1942.0, and 754.3 cm^{-1} even at low metal concentrations seems therefore to favor their assignment to the ammonia adducts $H_2MNH_2\cdot NH_3$.

Origins of the Products 4a−4c. While the origins of $M\cdot NH_3$, $HMNH_2$, and MNH_2, the primary products of the thermal and photochemical reactions occurring between a group 13 metal atom M and NH_3, are relatively clear, the reaction or reactions affording the secondary product H_2MNH_2 are less obvious. One mechanism involves the addition of the H atoms released in the photoreaction 3 to the subvalent metal compounds MNH_2 and $HMNH_2$, as in eq 4, for example. However, the knowledge that H_2 molecules undergo photoactivated addition to GaCl[42] or InCl[15] (eq 5) to give the trivalent product H_2MCl (M = Ga or In) suggests an alternative mechanism in which a similar reaction is induced between H_2 (formed by recombination of the H atoms) and the univalent metal amide MNH_2. Investigation of this second possibility was the primary motive for carrying out experiments in which the matrices were doped with both ammonia and dihydrogen. The addition of H_2 was certainly found to boost the yield of H_2MNH_2. Although this might seem to favor the second mechanism involving largely concerted photoaddition of H_2 to MNH_2, the presence of H_2 led also to the formation of the dihydride MH_2 and thence, on broad-band UV−visible photolysis, to the monohydride MH and H atoms;[10] it therefore provides an additional source of H atoms. Telling evidence that H atoms and not H_2 are the principal, possibly sole, means of access to H_2MNH_2 comes from an experiment involving a matrix containing Ga atoms together with NH_3 and D_2. Were D_2 addition the primary reaction, the main product would be D_2GaNH_2 readily recognizable by the strong IR absorptions near 1400 cm^{-1} due to its ν(Ga−D) modes. In the event, only weak absorptions were observed to build up in this region, whereas relatively strong bands were observed to develop near 1970 cm^{-1} (indicating that cleavage of an N−H bond is more readily achieved than cleavage of a D−D bond). It was also apparent that the yield of H_2GaNH_2 decreased almost to vanishing point when the matrix concentration of NH_3 was reduced by a factor of 10. Hence we conclude that H atoms

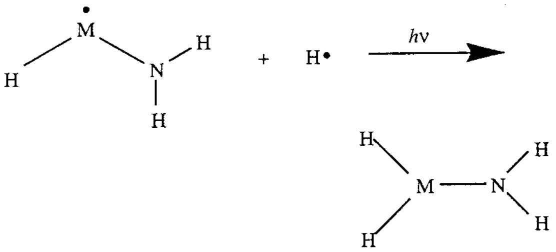

(4)

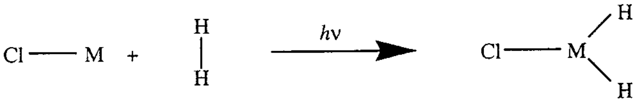

(5)

produced by broad-band UV−visible photolysis of $HMNH_2$ are the main begetters of H_2MNH_2 in a reaction sequence that plainly requires the activation of more than one NH_3 molecule.

Conclusions

The reactions that occur between Al, Ga, or In atoms and NH_3 have been investigated using the technique of matrix isolation to trap both the reagents and products and investigate their photochemistries. The various products have been identified and characterized primarily by their IR spectra. The response of the spectra to replacing $^{14}NH_3$ by $^{14}ND_3$ or $^{15}NH_3$ and to the natural presence of ^{69}Ga and ^{71}Ga and the vibrational properties simulated for the individual molecules by DFT calculations have played central roles in assessing the natures of these products.

The first product formed by the thermal reaction of the metal atoms with NH_3 is the adduct $M{\cdot}NH_3$ (M = Al, Ga, or In), which can be identified not only by its IR spectrum but also by a visible absorption band near 428 nm for Al/NH_3, near 440 nm for Ga/NH_3, and near 435 nm for In/NH_3. Irradiation with visible light having λ = ca. 436 nm brings about tautomerization of $M{\cdot}NH_3$ with insertion of the metal atom into one of the N−H bonds of ammonia to form the odd-electron amidometal hydride, $HMNH_2$. As in the reactions with H_2[10] and CH_4,[14] this change appears to be contingent on excitation of the metal atom from its ground ^2P to a ^2S or ^2D state; the visible absorption of the adduct probably represents the $^2S \leftarrow {}^2P$ transition of the coordinated M atom. The M(II) derivatives suffer photodissociation under the action of broad-band UV−visible light ($200 \le \lambda \le 800$ nm) with the formation of the univalent metal amide, MNH_2, and the release of H atoms. A secondary reaction brought about by these atoms involves addition to MNH_2 or $HMNH_2$ to produce trivalent amidoalane, -gallane or -indane, H_2MNH_2 (M = Al, Ga, or In). The H_2MNH_2 molecules are characterized by planar, ethene-like geometries with C_{2v} symmetry. The calculated M−N bond lengths follow the order $M{\cdot}NH_3 > H_3M{\cdot}NH_3 > MNH_2 > HMNH_2 \gtrsim H_2MNH_2 > HMNH$. As reported previously,[30] the barriers to rotation about the MN bond of H_2MNH_2 are calculated to be 161.9, 50.6, 65.7, and 51.5 kJ mol^{-1} for M = B, Al, Ga, and In, respectively, implying that π-interactions play quite a minor role in molecules of this sort, except when M = B. A fuller discussion of the observed and calculated properties of MNH_n molecules (n = 0−6), addressing inter alia the influences of π-bonding and bond polarity, will be presented elsewhere.[47]

Acknowledgment. The authors thank (i) the EPSRC for support of this research, including the purchase of equipment and the award of an Advanced Fellowship to T.M.G., and (ii) the Deutsche Forschungsgemeinschaft for the award of a postdoctoral grant to H.-J.H.

JA001313X

---

(47) Himmel, H.-J.; Downs, A. J.; Greene, T. M. *J. Chem. Soc., Dalton Trans.*, manuscript in preparation.